THE ASTROPHYSICAL JOURNAL, 452:652–670, 1995 October 20

ON COAGULATION AND THE STELLAR MASS SPECTRUM

ERIC J. ALLEN AND PIERRE BASTIEN
Montreal Star Formation Group, Département de Physique, Université de Montréal, C.P. 6128, Succ. A, Montréal, Québec, H3C 3J7, Canada; and Observatoire du Mont Mégantic
Received 1994 September 1; accepted 1995 May 1

ABSTRACT

The importance of coagulation in the making of the stellar mass spectrum is studied using two coagulation indicators and the model of Lejeune and Bastien. A search is made for correlations between these indicators and the physical characteristics of the four types of stellar groups investigated here: open clusters (54 cases), OB associations (16 cases), globular clusters (16 cases), and galaxies (13 cases). Although (1) coagulation is certainly not the only physical process which determines eventually the stellar mass spectrum and (2) the Lejeune and Bastien analytical solution describes only approximately the physics involved, we found that it fits the mass spectra extremely well. The fits are definitely much better than the usual power-law fits. The results show that coagulation seems to be pretty independent of the conditions at which it takes place. The means of the coagulation indicators for each type of stellar group are found to be quite close to each other (within the limits of uncertainty), which adds more weight to these results. It is also found that the effects of coagulation are difficult to show, at least for stellar groups with ages greater than $\cong 10^7$ yr. A method of assessing the amount of mass loss by the cluster is also described.

Subject headings: open clusters and associations: general — stars: formation — stars: luminosity function, mass function

1. INTRODUCTION

One of the most useful tools in the study of star formation is surely the stellar mass spectrum. Its many uses in this field of research have been extensively reviewed by Scalo (1986). Because the mass spectrum is the direct outcome of the processes that took place during the formation of a group of stars, it can tell us something about the importance of each one of these processes. Two of the main processes involved in the making of the stellar mass spectrum are fragmentation and coagulation. In most studies, each of these processes is dealt with separately, that is, either only one process occurs, or one starts after the other has finished (see Lejeune & Bastien 1986 for a brief review of the literature on these two formation processes; also, see Sorensen, Zhang, & Taylor 1987, Vigil & Ziff 1988, Ball & Carr 1990, Lin 1992, Sintes, Toral, & Chakrabarti 1992, Dubovskii, Galkin, & Stewart 1992, Simons 1993, Kamphorst & da Silva 1993, Saied & El-Wakil 1994, and Blackman & Marshall 1994 for details on the fragmentation and coagulation equation). How important is the influence of each process on the stellar mass spectrum can only be evaluated numerically if one has a model that has some physical sense. Ultimately, by knowing where, when, and how each process dominates, one could create a working model which deals with fragmentation and coagulation *at the same time*.

One model for coagulation was described by Silk & Takahashi (1979). They solved the coagulation equation analytically for three time-independent parameterizations of the coalescence rate and by assuming a Dirac-delta distribution of the mass of the initial fragments. Bastien (1981) then pointed out the importance of time during the coagulation process by comparing the mean collision time of a fragment of a given mass with any other to the free-fall time of that fragment. The ratio of these timescales was found to depend strongly on the mass of the fragment. Bastien concluded that coagulation dominates the high-mass end of the initial mass function, whereas another process, presumably fragmentation, must dominate its low-mass end ($m \lesssim 1\ M_\odot$).

The possibility that coagulation varies with time was addressed by Lejeune & Bastien (1986) with the finding of new solutions of the coagulation equation with a time-dependent coalescence rate. They found that the stellar mass spectrum cannot be reproduced by the coagulation equation when gravitational collapse of the fragments upon themselves is taken into account if the initial mass of the fragments is small, as is usually assumed. The only cases where significant evolution of the mass spectrum occurs was found to correspond to unrealistically large values of the coagulation rate.

The aim of the present paper is thus to verify these findings by comparing the stellar mass spectrum predicted by the work of Lejeune & Bastien with mass spectra of different stellar groups: open clusters, OB associations, globular clusters, and galaxies. We then compare our results with the physical characteristics of each of these groups in order to determine the conditions in which coagulation plays an important role.

It has been suggested in many reviews (see Elmegreen 1987, 1990, 1991) that it is not clear whether coagulation is responsible for the mass spectrum of molecular clouds and also whether this mass spectrum is directly related to the stellar one. This is mostly because other processes (such as stellar winds, for example) are also present, and they modify to some degree the stellar mass spectrum. Because the magnitude of the effects that these processes have on the transition between a *cloud* mass spectrum and a *stellar* mass spectrum is still not known, we are forced to assume that this transition is direct, i.e., the stellar mass spectrum is linked to the cloud mass spectrum in a one-to-one fashion. In any case, these problems will affect any comparison made between theoretical and experimental mass spectra until the effect is fully understood. We think that, although the coagulation-only model may be simple, it can still be used to find out the contribution of coagulation to the mass spectrum in various environments.

In § 2 we outline the basic concepts and definitions linked with coagulation, while § 3 is devoted to the method of analysis behind the results presented in the same section. We then concern ourselves (§ 4) with the search for correlations between the parameters calculated in § 3 for each case and the physical characteristics (age, metallicity, etc.) of each of these cases. A discussion of the results is given in § 5. In light of these results, we present our conclusions in § 6.

2. THEORY

We use the formalism defined by Scalo (1978) throughout this work, since it is the most widely used. The coagulation equation (CE) can be written:

$$\frac{\partial N(m, t)}{\partial t} = \frac{1}{2}\int_{m_l}^{m-m_l} \alpha(m', m-m', t)N(m', t)N(m-m', t)dm' - N(m, t)\int_{m_l}^{m_u-m_l} \alpha(m, m', t)N(m', t)dm' , \quad (1)$$

where $N(m, t)$ is the number density of fragments in the mass interval m to $m + dm$, $\alpha(m, m', t)$ is the coalescence rate, and m_l and m_u are respectively the lower and upper bounds on the mass of the fragments. The first integral gives the production of fragments of mass m due to collisions with fragments of mass m' and $m - m'$, with the factor $\frac{1}{2}$ to prevent counting a collision twice. The second integral represents the loss of a fragment of mass m due to its inelastic collision with another fragment.

Many types of analytical solutions of this equation have been found by various authors. The differences between these solutions come from the way the parameterization of the coalescence rate $\alpha(m, m', t)$ is done. Smoluchowski (1916) found a solution with α = constant, Safronov (1963) used $\alpha = \alpha_0(m + m')$ for his work, and Trubnikov (1971) added these previous parameterizations of the coalescence rate to his own to solve the CE in the more general case where $\alpha = \alpha_0 + \alpha_1(m + m') + \alpha_2 mm'$. Lejeune & Bastien (1986) then added a time dependency to α and found solutions independent of the mass as well as for $\alpha = \alpha_1(t)\,(m + m')$ [but not for $\alpha = \alpha_2(t)mm'$, since that would have no readily interpretable physical meaning].

We will start with their mass-dependent solution in its most general form, that is, with no specific time dependency for the coalescence rate:

$$N(m, t) = \frac{\rho[c(t)/N_0]}{m_0 m[1 - c(t)/N_0]} \exp\left\{-\frac{m[1 - c(t)/N_0]}{m_0}\right\} \times \left\{\frac{m[1 - c(t)/N_0]}{m_0}\right\}^{m/m_0} \frac{1}{(m/m_0)!} , \quad (2)$$

where an initial mass spectrum of the form

$$N(m, 0) = N_0\,\delta(m - m_0) \quad (3)$$

has been assumed. Here N_0 is the initial number of fragments of mass m_0 per unit volume; hence the total initial density is $\rho = N_0 m_0$. We must point out that the dimensions of N are not the same as those of N_0. This happens because we use the Dirac delta function $\delta(m - m_0)$, which has the dimension of the inverse of mass. Thus, the dimensions of N_0 must be those of a pure number per unit of volume in order for N to become the number density of fragments.

The parameter $c(t)$ is defined as

$$c(t) = N_0 \exp\left[-\alpha_0 N_0 m_0 \int_0^t \alpha(t')dt'\right] , \quad (4)$$

and we see that it depends on the choice made for the parameterization of $\alpha(t)$.

Equation (2) can be written more clearly if we define $C = c(t)/N_0$ and $M = m/m_0$, two nondimensional variables:

$$\frac{mN(m, t)}{N_0} = \frac{C}{1 - C}[M(1 - C)]^M \frac{1}{M!} \exp[-M(1 - C)] , \quad (5)$$

and we can see that, in this form, it is dimensionally equivalent to the *mass function* $\xi(\log (m/m_\odot))$ as defined by Scalo (1986). It is now straightforward to compare the predictions of this equation with astronomical observations. First, let us investigate what the two free parameters C and m_0 can tell us about the amount of coagulation involved in the cases analyzed.

2.1. *Coagulation Indicators*

From equation (4) we see that the form of the function $c(t)$ depends on the way the coagulation parameter varies with time, and we have made no assumptions about this so far. The coagulation parameter is the product of the cross section and the relative velocity of two colliding fragments, averaged over the velocity distribution of the fragments. Since the fragments are collapsing on themselves, their cross section should decrease with time or, at worst, stay constant when they stop collapsing. As for the relative velocity of the fragments, it should stay below a limit, mainly the average escape velocity of the cluster.[1] The overall picture should be that $\alpha(t)$ either decreases or at worst stays constant with time. Thus, the value of the exponential should follow the same behavior.

Now, if we consider the dimensionless parameter C defined earlier, we can safely predict that it should decrease with time if some coagulation is occurring [that behavior can be assessed without the considerations of the last paragraph just by knowing that $\alpha(t)$ is positively defined and that the exponential is negative] or that it should have a constant value smaller than unity and constant if $\alpha \neq \alpha(t)$. Conversely, if there is no coagulation, the value of C will be exactly equal to unity.

From this little digression we retain the result that the more coagulation there is, the smaller the value of C. In simpler terms, we can also say that C is the fraction of fragments that remain after coagulation has taken place for a certain time t. Thus, the amount of coagulation that occurred in a certain group of stars can be assessed with the numerical value of C calculated for this group (we will see in the next section how this is done in the present work).

Another way to estimate numerically the amount of coagulation that occurred is simply comparing m_0, the initial mean mass of the fragments, with the value $\bar{m}$ it has when the observation is made. Obviously, $\bar{m}$ should be larger than m_0 if coagulation has taken place. Therefore, the ratio $\bar{m}/m_0$ is another numerical indicator of coagulation.

We expect a direct correlation between C and $\bar{m}/m_0$, since

$$\frac{\bar{m}}{m_0} = \frac{(M_{\rm tot}/N)_{t'=\rm today}}{(M_{\rm tot}/N)_{t'=0}} \simeq \frac{N_0}{N_{\rm today}} = C^{-1} \quad (6)$$

if we neglect any change of mass (by stellar evolution and/or by evaporation of less massive star, or by capture). However, if we are to take into account evaporation and mass loss, we expect the proportionality constant to be smaller than unity, that is,

[1] Of course, some fragments will have a velocity equal to or greater than the escape velocity of the cluster, but these will not show on the observed mass spectrum of actual clusters.

the slope of the relationship between $\bar{m}/m_0$ and C^{-1} will be flatter. Conversely, any input of mass (i.e., stellar capture) will give a slope greater than unity.

It is interesting to know that we can evaluate the amount of mass loss in the cluster using the two coagulation indicators (CIs). We want to know the ratio of the total mass of the cluster as it is today and as it was at its formation;[2] this ratio is given by equation (6) as

$$\frac{(M_{\rm tot})_{t'={\rm today}}}{(M_{\rm tot})_{t'=0}} = \frac{\bar{m}}{m_0}\, C\,. \qquad (7)$$

The amount of mass loss can thus be evaluated for each cluster without making any assumptions about the process that stripped the cluster of its *star mass*. If this loss is a constant for all clusters, then we should see a *direct* relationship between C and $\bar{m}/m_0$. In other words, C should be *inversely* proportional to $\bar{m}/m_0$. We will see in the next section that this is not exactly the case (although the interpretation will be looked at in more depth in an upcoming paper).

3. RESULTS

The method of analysis is simple. We first searched the literature for initial mass functions (IMFs) or present-day mass functions (PDMF) that could be used for this project. Because the normalization of these IMFs is quite arbitrary and varies with the authors, we had to find one that was general enough to be used for all types of clusters and that minimized the loss of information about the individual characteristics of each one. For this purpose, we treated the mass spectrum $f(m)$ as a probability function, so that

$$\int_{m_l}^{m_u} f(m) dm = 1\,. \qquad (8)$$

Recall, though, that we are using the mass *function* $F(\log m)$ in our calculations; it is related to the mass *spectrum* $f(m)$ by (Scalo 1986)

$$F(\log m) = (\ln 10) m f(m)\,. \qquad (9)$$

Hence,

$$\int_{\log m_l}^{\log m_u} F(\log m) d(\log m) = \int_{m_l}^{m_u} (\ln 10) m f(m)\, \frac{dm}{m \ln 10}\,, \qquad (10)$$

which, by virtue of equation (8), gives

$$\int_{\log m_l}^{\log m_u} F(\log m) d(\log m) = 1\,. \qquad (11)$$

We thus normalized all the mass functions according to equation (11) and then fitted equation (5) to the data by varying the two free parameters C and m_0 until the χ^2 was minimized. All the data points available were used for the curve fitting.

The results are shown in Table 1 for open clusters, in Table 3 for OB associations and two molecular clouds, in Table 5 for globular clusters, and in Table 7 for galaxies and the local IMF and PDMF. In all four tables, column (1) gives the name of the object; column (2) lists the number of data points used in the calculations; columns (3) and (4) contain, respectively, the best-fit initial mean mass of the stars in solar mass and its present-day value; and column (5) consists of the ratio of the present-day mean mass of the stars to its initial value. Column (6) gives the best-fit value of C. Column (7) gives the total χ^2, and column (8) lists the corresponding probability that this fit represents reality. Finally, column (9) gives the source for the data used in the computations.

Table 2, 4, 6, and 8 show the results of a simple linear regression on the mass spectra for, respectively, open clusters, OB associations and two molecular clouds, globular clusters, and galaxies. Column (1) gives the name of the object; column (2) gives the power-law index, with its associated standard deviation given in column (3). Columns (4) and (5) contain, respectively, the total χ^2 and the corresponding probability that the fit represents reality. Column (6) lists the source of the data used for computation. The equation used for the linear regression was (Salpeter 1955)

$$\frac{mN(m, t)}{N_0} = m^{\Gamma}\,, \qquad (12)$$

where Γ is simply the slope of the line in a log-log plot.

The words "mean inner" and "mean outer" in Tables 1 and 2 stand for mass spectra composites of the inner and outer parts of our Galaxy (see Vázquez & Feinstein 1989 for more details). For ω Centauri, two sets of data obtained at two different observatories were used (Los Campanas [LC] and the European Southern Observatory [ESO]). In Tables 7 and 8 the word "local" refers to our Galaxy, "inner" stands for the inner part of our Galaxy, "outer" is obviously for the outer part, and "MW spheroid" means Milky Way spheroid. We should also point out that the two objects called ρ Oph found in Tables 1 and 2 and in Tables 3 and 4 are indeed two different types of objects (one is a very young open cluster found near the star ρ Oph, while the other is a molecular cloud found in the same region; see Comeron et al. 1993 and Nozawa et al. 1991 for details).

It is worth noting that we had to omit a few data points in some best-fit calculations, since they prevented us from finding a converging set of best-fit values. The mass spectrum of these clusters (in all cases open clusters) all had an important turnover in the low-mass range that the coagulation model could not fit properly at the same time as the high-mass range. We thus omitted some points of the turnover to obtain a best fit of the high-mass end of the spectrum. The number of remaining points was large enough to give meaningful results. The χ^2 and corresponding probability of the fit were calculated with the reduced mass spectrum, and the clusters that were affected by this method are indicated in Tables 1 and 2 by an asterisk next to the probability of the fit value.

Table 9 contains the Pearson correlation coefficient for the correlation between the two CIs C and $\bar{m}/m_0$ for each type of stellar cluster and the number of data points used in the calculation.

We give in Table 10 the extreme values for the C parameter along with its weighted mean and standard deviation for each type of stellar group. We can see that the mean values and their standard deviations are quite close (keep in mind that the four cases studied have wildly different ages and initial conditions), which is surprising unless one believes in a universal IMF or in the fact that coagulation is a strictly stochastic process.

Table 11 contains the same data as Table 10, but for the ratio $\bar{m}/m_0$. Again the mean values are somewhat close within the limits of uncertainty even though the extremum values are

[2] Here we calculate the total mass in terms of *stars*, and we neglect the leftover gas and dust.

TABLE 1

OPEN CLUSTERS: FITS OF THE COAGULATION MODEL

Name (1)	Number of points (2)	m_0 (3)	$\bar{m}$ (4)	$\bar{m}/m_0$ (5)	C (6)	χ^2 (7)	Probability[a] (8)	Reference (9)
NGC 103	10	0.255	1.65	6.47	0.417	4.765	0.7824	1
NGC 129	8	2.16	2.11	0.978	0.986	0.446	0.9940*	2
NGC 330	9	3.51	3.36	0.957	0.983	0.306	0.9999	3
NGC 436	9	1.28	3.13	2.45	0.662	0.439	0.9996	1
NGC 457	9	1.50	3.22	2.14	0.798	0.697	0.9984	1
NGC 581	8	3.80	4.52	1.19	0.906	0.676	0.9950	4
NGC 581	11	0.421	1.57	3.73	0.557	3.915	0.9169	1
NGC 654	6	5.32	6.12	1.15	0.915	1.519	0.8232	4
NGC 659	14	0.807	3.48	4.312	0.581	1.541	0.9968*	1
NGC 663	13	0.512	2.60	5.08	0.484	2.297	0.9972	1
NGC 1342	7	1.84	1.65	0.899	0.980	0.282	0.9980	5
NGC 1528	9	1.63	1.48	0.909	0.986	0.921	0.9960	5
NGC 1647	9	1.69	1.73	1.02	0.992	3.557	0.8292	5
NGC 1711	10	2.35	2.16	0.920	0.996	0.542	0.9998	3
NGC 1711	9	3.65	3.30	0.904	0.979	0.272	0.9999	6
NGC 1778	7	1.93	2.64	1.37	0.863	1.602	0.9010	4
NGC 1831	12	1.27	1.12	0.885	0.999	0.545	1.0000	3
NGC 2010	10	2.38	2.36	0.992	0.977	1.464	0.9933	3
NGC 2164	8	3.09	2.72	0.880	0.977	0.322	0.9994	6
NGC 2214	9	2.99	2.77	0.928	0.970	1.116	0.9927	6
NGC 2269	6	0.511	1.63	3.19	0.575	0.175	0.9964	7
NGC 2281	11	1.26	1.37	1.09	0.929	3.199	0.9559	5
NGC 2420	8	1.38	0.95	0.691	0.968	3.639	0.7254	8
NGC 2539	3	2.81	2.39	0.850	0.991	0.386	0.5344	4
NGC 3293	9	0.583	5.01	8.59	0.435	1.190	0.9912	9
NGC 6334f4	16	2.359	8.05	3.412	0.819	3.502	0.9823*	10
NGC 6334f5	13	0.128	6.36	49.8	0.143	3.419	0.9840	10
NGC 6334g1	16	2.708	7.35	2.714	0.701	1.639	0.9960*	10
NGC 6334g2	15	0.086	7.37	86.0	0.132	3.556	0.9951	10
NGC 6334g3	13	0.113	4.37	38.7	0.180	4.173	0.9646	10
NGC 6334g4	16	0.806	6.17	7.66	0.417	2.602	0.9996	10
NGC 6530	8	4.69	5.89	1.26	0.892	0.698	0.9945	4
NGC 6611	9	14.00	22.98	1.64	0.788	1.012	0.9946	4
NGC 6611	6	8.03	11.04	1.38	0.965	0.577	0.9656	11
NGC 6633	7	6.76	1.54	0.228	0.915	3.006	0.6991	5
NGC 6823	11	9.79	24.30	2.48	0.669	1.809	0.9941	4
NGC 6913	7	4.64	5.77	1.25	0.999	1.885	0.8648	4
NGC 7790	10	1.528	2.66	1.741	0.816	0.437	0.9996*	1
Be 42	4	2.06	1.03	0.499	0.939	0.018	0.9912	12
H4	7	1.27	1.07	0.843	0.999	1.592	0.9022	3
Hyades	9	0.896	0.97	1.083	0.950	0.906	0.9237*	13
IC 1805	11	7.61	10.97	1.44	0.927	1.078	0.9992	4
King 11	8	1.88	1.03	0.548	0.942	0.051	1.0000	12
LW 79	8	1.46	1.30	0.892	0.985	5.769	0.4496	3
M25	7	2.16	1.91	0.886	0.982	1.221	0.9429	5
M35	6	1.87	2.28	1.22	0.846	1.464	0.8330	14
Mel. 111	7	1.79	1.48	0.828	0.900	3.183	0.6717	15
N59A	5	8.87	10.43	1.18	0.940	0.181	0.9806	16
Pleiades	16	0.131	0.22	1.679	0.721	0.325	1.0000*	17
Praesepe	7	0.302	1.10	3.64	0.608	5.048	0.4101	13
ρ Oph	6	0.017	1.21	71.18	0.644	1.746	0.7824	18
RCW 108	11	0.470	4.35	9.26	0.318	0.318	0.9495	19
TR 1	6	3.80	4.21	1.11	0.919	0.919	0.9552	4
TR 1	9	0.645	2.07	3.21	0.581	2.378	0.9360	1
Mean inner	8	9.76	20.86	2.14	0.758	0.206	0.9998	20
Mean outer	8	9.31	17.67	1.90	0.851	0.343	0.9993	20

[a] Asterisks denote fits that were made by omitting some points in the lower mass range, and, consequently, the χ^2 and probabilities were calculated without these points. The number of points used for the calculations was 7 out of 8 (7/8) for NGC 129, 11/14 for NGC 659, 13/16 for NGC 6334f4, 11/16 for NGC 6334g1, 9/10 for NGC 7790, 6/9 for the Hyades, and 13/16 for the Pleiades. See text for more details.

REFERENCES.—(1) Phelps & Janes 1993; (2) Lee & Lee 1984; (3) Mateo 1988; (4) Sagar et al. 1986; (5) Francic 1989; (6) Sagar & Richtler 1991; (7) Bhattacharjee & Williams 1980; (8) Leonard 1988; (9) Herbst & Miller 1982; (10) Straw et al. 1989; (11) Hillenbrand et al. 1993; (12) Aparicio et al. 1991; (13) Lee & Kim 1983; (14) Leonard & Merritt 1989; (15) Bounatiro & Arimoto 1992; (16) Armand et al. 1992; (17) Hambly et al. 1991; (18) Comeron et al. 1993; (19) Straw et al. 1987; (20) Vázquez & Feinstein 1989.

TABLE 2

OPEN CLUSTERS: FITS OF THE POWER-LAW MODEL

Name (1)	Γ (2)	σ_Γ (3)	χ^2 (4)	Probability[a] (5)	Reference (6)
NGC 103	−0.93	0.33	964.37	0.0000	1
NGC 129	−2.74	0.31	1.04	0.9592*	2
NGC 330	−3.48	0.26	26.27	0.0005	3
NGC 436	−0.68	0.18	166.68	0.0000	1
NGC 457	−1.03	0.11	183.43	0.0000	1
NGC 581	−1.52	0.14	3.10	0.7966	4
NGC 581	−1.28	0.28	1198.58	0.0000	1
NGC 654	−1.84	0.70	36.36	0.0000	4
NGC 659	−0.90	0.15	726.69	0.0000*	1
NGC 663	−1.06	0.19	169.72	0.0000	1
NGC 1342	−2.16	0.17	1.08	0.9562	5
NGC 1528	−2.84	0.23	12.18	0.0949	5
NGC 1647	−1.88	0.60	60.66	0.0000	5
NGC 1711	−3.30	0.17	11.20	0.1906	3
NGC 1711	−2.87	0.33	28.70	0.0002	6
NGC 1778	−1.05	0.44	12.68	0.0266	4
NGC 1831	−5.32	0.39	32.00	0.0004	3
NGC 2010	−3.82	0.69	167.62	0.0000	3
NGC 2164	−2.44	0.31	17.31	0.0082	6
NGC 2214	−2.55	0.51	47.22	0.0000	6
NGC 2269	−1.22	0.32	10.02	0.0401	7
NGC 2281	−1.60	0.43	29.14	0.0006	5
NGC 2420	−0.69	0.93	53.43	0.0000	8
NGC 2539	−3.20	1.39	13.58	0.0002	4
NGC 3293	−0.78	0.14	2.98	0.8865	9
NGC 6334f4	−0.79	0.20	14.04	0.2307*	10
NGC 6334f5	−0.08	0.28	27.64	0.0367	10
NGC 6334g1	−1.36	0.25	3.38	0.9475*	10
NGC 6334g2	−0.36	0.25	23.81	0.0329	10
NGC 6334g3	−0.83	0.30	29.76	0.0017	10
NGC 6334g4	−0.84	0.22	25.41	0.0307	10
NGC 6530	−1.49	0.30	3.48	0.7470	4
NGC 6611	−0.87	0.25	9.58	0.2137	4
NGC 6611	−1.53	0.22	3.75	0.4411	11
NGC 6633	−0.04	0.79	43.10	0.0000	5
NGC 6823	−0.77	0.20	17.09	0.0473	4
NGC 6913	−1.36	0.58	62.99	0.0000	4
NGC 7790	−1.54	0.13	224.16	0.0000*	1
Be 42	−0.27	0.19	0.62	0.7331	12
H4	−4.59	1.08	21.67	0.0006	3
Hyades	−2.95	0.95	39.94	0.0000*	13
IC 1805	−1.45	0.24	3.45	0.9436	4
King 11	−0.41	0.11	1.16	0.9786	12
LW 79	−2.68	1.22	107.78	0.0000	3
M25	−2.51	0.61	16.06	0.0067	5
M35	−1.05	0.40	24.73	0.0001	14
Mel 111	−0.38	0.77	29.07	0.0000	15
N59A	−1.84	0.26	0.31	0.9573	16
Pleiades	−0.84	0.12	5.40	0.9103*	17
Praesepe	−1.24	0.98	47.93	0.0000	13
ρ Oph	−0.45	0.56	2.92	0.5716	18
RCW 108	−0.45	0.29	19.48	0.0214	19
TR 1	−1.04	0.31	2.64	0.6193	4
TR 1	−0.85	0.32	1349.86	0.0000	1
Mean inner	−1.28	0.14	6.68	0.3511	20
Mean outer	−1.39	0.08	0.8253	0.9914	20

[a] Asterisks denote fits that were made by omitting some points in the lower mass range, and, consequently, the χ^2 and probabilities were calculated without these points. The number of points used for the calculations were 7/8 for NGC 129, 11/14 for NGC 659, 13/16 for NGC 6334f4, 11/16 for NGC 6334gl, 9/10 for NGC 7790, 6/9 for the Hyades, and 13/16 for the Pleiades. See text for more details.

REFERENCES.—(1) Phelps & Janes 1993; (2) Lee & Lee 1984; (3) Mateo 1988; (4) Sagar et al. 1986; (5) Francic 1989; (6) Sagar & Richtler 1991; (7) Bhattacharjee & Williams 1980; (8) Leonard 1988; (9) Herbst & Miller 1982; (10) Straw et al. 1989; (11) Hillenbrand et al. 1993; (12) Aparicio et al. 1991; (13) Lee & Kim 1983; (14) Leonard & Merritt 1989; (15) Bounatiro & Arimoto 1992; (16) Armand et al. 1992; (17) Hambly et al. 1991; (18) Comeron et al. 1993; (19) Straw et al. 1987; (20) Vázquez & Feinstein 1989.

dissimilar for each case. Still, the open clusters and the OB associations seem to have experienced more coagulation than the globular clusters, as the mean of both CIs shows us.

We give in Table 12 the mean values of the probability of the fit for the coagulation and power-law models for each type of stellar group, along with its standard deviation. Columns (2) and (3) are for the coagulation model, and columns (4) and (5) are for the power-law model. As can be seen, the coagulation model fits the data quite well, especially for globular clusters. We cannot say the same for the power-law model.

We plot in Figure 1 six cases where the coagulation model fits the data quite well. The first five are open clusters, and the last one is a globular cluster. In order to appreciate the flexibility of the model, we have put all the open cluster figures on the same scale. One can see that the model can fit a wide range of mass with only two adjustable parameters, mainly C and m_0. The error bars for the mass come from the source of the data, while the ones for ξ are simply the square root of the number of stars. For comparison purposes we have also included the best-fit line for the power-law model.

It is clear from these figures that the coagulation model is significantly better at fitting the data than a simple power law. The high-mass end, where coagulation is believed to have a greater influence (Bastien 1981), is very well fitted by the model, whereas the low-mass end is less so. In three cases (NGC 663, NGC 7790, and the Pleiades) the model overestimates the number of low-mass stars, while in another one (NGC 663) this number is underestimated. The overestimate can be surprising at first glance, since coagulation implies a lower number of fragments. However, it can easily be explained by at least two phenomena. First of all, it is possible that there is an observing bias, i.e., the number of faint stars (and, by extension, the number of less massive ones) detectable by instruments depends strongly on the distance of the cluster. Hence, the apparent turnover in the data can be overestimated by this selection effect and thus give a smaller number of stars than the coagulation model predicts.

Second, there is some evaporation of stars during the dynamical relaxation of the cluster. This phenomenon is known to be more important for low-mass stars (see Johnstone 1993). Hence the evaporation of low-mass stars will give the turnover a greater magnitude than predicted by the coagulation model. It is also possible that the observed turnover is a result of a combination of these two explanations with a real turnover of the IMF.

As for the underestimate of the number of low-mass stars by the coagulation model, it simply shows that we should include fragmentation in the modeling of the mass spectrum. This also supports the conclusion by Bastien (1981) about the range where coagulation is more important and where fragmentation takes over. Notice that the model departs from the data at around the same value of mass, mainly $\approx 1\ M_\odot$.

Regarding the expected relationship between $1/C$ and $\bar{m}/m_0$, we found that there definitely is one, as can be seen in Figure 2 and in the results of Table 9. In Figure 2*a* we have included every type of star cluster studied in this paper. Figure 2*b* is a blowup of Figure 2*a*. In both cases, the solid line represents the expected relationship if no mass loss had occurred. It is clear that some mass loss has occurred in virtually every type of star cluster and that its magnitude seems independent of the type. Because it is not the main purpose of this work to study mass-loss processes, we refer to a subsequent paper for a detailed analysis of this topic.

TABLE 3

OB ASSOCIATIONS AND MOLECULAR CLOUDS: FITS OF THE COAGULATION MODEL

Name (1)	Number of Points (2)	m_0 (3)	$\bar{m}$ (4)	$\bar{m}/m_0$ (5)	C (6)	χ^2 (7)	Probability (8)	Reference (9)
α Persei	12	2.91	3.19	1.10	0.815	3.291	0.9737	1
Centaurus	14	3.54	5.45	1.54	0.653	5.827	0.9245	1
Cygnus OB2	6	9.31	21.38	2.30	0.677	0.321	0.9884	2
η Car	7	9.10	20.31	2.23	0.682	0.279	0.9980	3
LH 9	10	0.506	12.46	24.62	0.211	3.029	0.9325	4
LH 10	11	2.25	15.91	7.08	0.376	1.764	0.9947	4
LH 117	6	8.90	12.04	1.35	0.891	0.169	0.9966	5
LH 118	5	8.72	11.30	1.30	0.914	0.247	0.9697	5
NGC 346	6	8.46	12.36	1.46	0.871	0.274	0.9915	6
NGC 2264	12	2.05	3.55	1.73	0.865	0.656	1.0000	7
Orion a	13	3.72	4.31	1.16	0.884	1.865	0.9989	1
Orion b	14	1.54	3.92	2.54	0.614	8.363	0.7561	1
Orion b2	12	2.79	3.89	1.40	0.753	6.106	0.8063	1
Orion c	14	3.04	3.86	1.27	0.857	3.056	0.9951	1
Orion	10	4.14	3.87	0.935	0.936	1.155	0.9971	8
Scorpius	17	1.48	4.63	3.13	0.503	6.794	0.9631	1
L1630	8	1.34	81.96	61.16	0.132	0.631	0.9959	9
ρ Oph	8	25.70	8.23	0.320	0.982	2.027	0.9172	10

REFERENCES.—(1) Claudius & Grosbøl 1980; (2) Massey & Thompson 1991; (3) Massey & Johnson 1993; (4) Parker et al. 1992; (5) Massey et al. 1989a; (6) Massey et al. 1989b; (7) Sagar et al. 1986; (8) Tarrab 1982; (9) Lada et al. 1991a; (10) Nozawa et al. 1991.

4. CORRELATIONS

As we saw in Table 10, the standard deviation of C is quite small compared to that for the spectral index, which points toward a universal IMF. In order to investigate this assumption in more detail, we searched for correlations between the two CIs described earlier and other physical characteristics of the different stellar groups studied in this paper. We feel that the CIs are better suited for correlation searches because they do not depend on the mass range where the fit is made, whereas the power-law model gives values of the slope Γ that depend strongly on the mass range. In this sense, the coagulation model makes it easier to compare two mass spectra whose mass ranges are not the same; it is a powerful instrument in the search for correlations. The power-law model does not permit this, since one cannot find a mass range common to all cluster mass spectra.

The results of this correlation search are summarized in Tables 13–16 for open clusters, OB associations, globular clusters, and galaxies, respectively. Column (1) gives the parameters used in the search; columns (2) and (3) contain, respectively, the Pearson product-moment correlation r-coefficient for C and $\bar{m}/m_0$, with the number of data points used for each case in column (4). The following subsections describe these results for each type of stellar cluster in more detail.

TABLE 4

OB ASSOCIATIONS AND MOLECULAR CLOUDS: FITS OF THE POWER-LAW MODEL

Name (1)	Γ (2)	σ_Γ (3)	χ^2 (4)	Probability (5)	Reference (6)
α Persei	−0.57	0.36	53.16	0.0000	1
Centaurus	0.05	0.40	54.41	0.0000	1
Cygnus OB2	−0.58	0.23	2.34	0.6733	2
η Car	−0.88	0.13	2.41	0.7901	3
LH 9	−0.41	0.37	21.60	0.0057	4
LH 10	−0.33	0.24	15.10	0.0882	4
LH 117	−1.77	0.18	2.97	0.5621	5
LH 118	−1.75	0.22	2.43	0.4888	5
NGC 346	−1.69	0.23	1.41	0.8430	6
NGC 2264	−1.05	0.15	4.84	0.9013	7
Orion a	−1.15	0.26	28.85	0.0024	1
Orion b	−0.92	0.45	80.26	0.0000	1
Orion b2	−0.56	0.44	76.15	0.0000	1
Orion c	−1.27	0.28	37.17	0.0002	1
Orion	−1.30	0.21	8.13	0.4206	8
Scorpius	−0.33	0.30	61.63	0.0000	1
L1630	−0.09	0.17	3.70	0.7166	9
ρ Oph	−1.08	0.26	1769.38	0.0000	10

REFERENCES.—(1) Claudius & Grosbøl 1980; (2) Massey & Thompson 1991; (3) Massey & Johnson 1993; (4) Parker et al. 1992; (5) Massey et al. 1989a; (6) Massey et al. 1989b; (7) Sagar et al. 1986; (8) Tarrab 1982; (9) Lada et al. 1991a; (10) Nozawa et al. 1991.

4.1. *Open Clusters*

There are many papers on the subject of correlations between the spectral index (x, Γ or η) and other attributes of open clusters. Taff (1974) examined the possibility that the spectral index is linked with the richness or concentration class of the cluster and found no clear evidence for that assumption. We looked for a possible correlation between C and $\bar{m}/m_0$ versus the concentration and richness classes[3] and arrived at the same conclusion: there is no statistical evidence against a universal IMF in the case of richness or concentration classes.

Burki & Maeder (1976) and Burki (1977) investigated the IMF and its variations with the diameter of the cluster as well as with its position in the Galaxy. They found that the mean diameter of the very young ($t < 1.5 \times 10^7$ yr) open clusters is a direct function of the distance to the center of the Galaxy. Mainly, the means of the diameters are 4.7 ± 0.9 pc at $R = 8.5$ kpc and 9.9 ± 1.6 pc at $R = 11.5$ kpc.

[3] All the data on the overall characteristics of open clusters come from the catalog of Lyngå (1987).

TABLE 5

GLOUBULAR CLUSTERS: FITS OF THE COAGULATION MODEL

Name (1)	Number of Points (2)	m_0 (3)	$\bar{m}$ (4)	$\bar{m}/m_0$ (5)	C (6)	χ^2 (7)	Probability (8)	Reference (9)
M3	10	0.09	0.30	3.464	0.588	1.196	0.9967	1
M5	21	0.40	0.39	0.965	0.910	1.831	1.0000	2
M12	15	1.75	0.53	0.303	0.878	0.4185	1.0000	3
M13	9	0.59	0.50	0.847	0.971	0.2650	0.9999	4
M15	11	0.62	0.48	0.775	0.964	0.166	1.0000	5
M30	15	0.37	0.36	0.963	0.961	1.037	1.0000	6
M71	14	0.32	0.35	1.106	0.867	2.054	0.9993	7
NGC 3201	8	0.84	0.56	0.666	0.960	0.197	0.9999	8
NGC 5053 global	8	1.06	0.64	0.603	0.989	0.713	0.9942	9
NGC 5053 inner	8	1.24	0.64	0.516	0.983	0.534	0.9974	9
NGC 5053 outer	10	0.71	0.56	0.779	0.994	0.410	0.9999	9
NGC 6171	7	7.06	0.69	0.097	0.984	0.061	1.0000	10
NGC 6397	16	0.22	0.32	1.442	0.762	1.655	1.0000	11
NGC 6752	14	0.22	0.24	1.087	0.995	3.418	0.9918	2
ω Cen LC	14	0.25	0.27	1.052	0.996	3.484	0.9911	2
ω Cen ESO	14	0.29	0.29	1.025	0.929	1.773	0.9997	2

REFERENCES.—(1) Da Costa & Freeman 1976; (2) Richer et al. 1991; (3) Sato et al. 1989; (4) Pryor et al. 1986; (5) Durrell & Harris 1993; (6) Piotto et al. 1990; (7) Richer et al. 1990; (8) Brewer et al. 1993; (9) Fahlman et al. 1991; (10) Ferraro & Piotto (1992); (11) Fahlman et al. 1989.

They interpreted this result in terms of the positive derivative of the Jeans radius with respect to the distance from the Galactic center due in part to the decrease of the mean gas density with R. They in turn determined that the proportion of massive stars in a given cluster follows the variation of the cluster's diameter; that is, the proportion of high-mass stars is higher for clusters with a big diameter. This result, joined with the preceding one about the variation of diameter with Galactocentric distance, gives the important result that the proportion of massive stars in a cluster is a direct function of the distance to the center of the Galaxy. That this result comes from either a difference in the *fragmentation* rate *or* a difference in the *coagulation* rate is difficult to answer, since this would require a dual analysis of both processes at the same time; but we can look for a similar behavior of the two coagulation indicators and see what it tells us.

TABLE 6

GLOBULAR CLUSTERS: FITS OF THE POWER-LAW MODEL

Name (1)	Γ (2)	σ_Γ (3)	χ^2 (4)	Probability (5)	References (6)
M3	−0.90	0.38	12.90	0.1152	1
M5	−1.25	0.11	10.13	0.9497	2
M12	0.23	0.10	3.81	0.9931	3
M13	−1.83	0.22	3.81	0.8010	4
M15	−1.52	0.18	7.34	0.6016	5
M30	−2.04	0.11	3.41	0.9960	6
M71	−1.04	0.15	14.94	0.2447	7
NGC 3201	−0.95	0.14	98.62	0.0000	8
NGC 5053 global	−1.45	0.46	28232.80	0.0000	9
NGC 5053 inner	−0.95	0.39	24714.70	0.0000	9
NGC 5053 outer	−2.86	0.23	3206.16	0.0000	9
NGC 6171	0.50	0.16	2408.68	0.0000	10
NGC 6397	−0.52	0.10	4.28	0.9935	11
NGC 6752	−1.80	0.18	56.81	0.0000	2
ω Cen LC	−2.04	0.21	45.80	0.0000	2
ω Cen ESO	−1.78	0.15	9.47	0.6620	2

REFERENCES.—(1) Da Costa & Freeman 1976; (2) Richer et al. 1991; (3) Sato et al. 1989; (4) Pryor et al. 1986; (5) Durrell & Harris 1993; (6) Piotto et al. 1990; (7) Richer et al. 1990; (8) Brewer et al. 1993; (9) Fahlman et al. 1991; (10) Ferraro & Piotto 1992; (11) Fahlman et al. 1989

As one can assess from Table 13, the coagulation parameters show no clear variation with distance from the Galactic center for clusters younger than 1.5×10^7 yr, and our sample covers $R \cong 5.9$ kpc to $R \cong 10.2$ kpc. Certainly the Pearson coefficient for C is high, but it is not supported by the other coagulation indicator. Furthermore, we only have seven clusters which satisfy the youth criterion in our analysis. So we must conclude that coagulation is a pretty constant process throughout our Galaxy and that the variations found by Burki (1977) and Burki & Maeder (1976) cannot be explained by it. This result is also supported by the absence of correlation between the linear diameter of the cluster and the amount of coagulation (see Table 13). We did the same analysis for all the clusters in our sample and arrived at the same conclusion. Surprisingly, we do not find any correlation between the diameter of a cluster and its distance from the center of the Galaxy with the clusters used in our study, either young or old.

Interestingly enough, when we compare the mean inner mass spectrum of open clusters and its corresponding mean in the outer part of the Galaxy (as published by Vázquez & Feinstein 1989), we find the CIs give more coagulation for the inner part of the Galaxy than for its outer part. If we do the same for the open clusters of this paper, we find the opposite result (inner Galaxy: $\langle C \rangle = 0.800$, $\langle \bar{m}/m_0 \rangle = 2.177$; outer Galaxy: $\langle C \rangle = 0.859$, $\langle \bar{m}/m_0 \rangle = 1.529$). We feel that the data of Vázquez & Feinstein is better for this purpose, since they had 16 clusters for the outer Galaxy results and 26 for the inner Galaxy. We had more clusters for the outer part analysis (29 open clusters) but considerably less for the inner part (only five clusters). Thus we cannot compare our two values the way they did. We can, however, compare our *outer* values with the ones obtained from the analysis of their *inner* data. We find that there seems to be more coagulation in the inner part than in the outer part, in agreement with what we got from the analysis of Vázquez & Feinstein's data.

So we get mixed results concerning a possible variation of coagulation in the plane of the Galaxy. If we simply look for a relationship between the CIs and the distance from the center of the Galaxy, we find nothing. If we look at the mean values of

TABLE 7

GALAXIES: FITS OF THE COAGULATION MODEL

Name (1)	Number of Points (2)	m_0 (3)	$\bar{m}$ (4)	$\bar{m}/m_0$ (5)	C (6)	χ^2 (7)	Probability (8)	Reference (9)
Local IMF	23	0.14	0.58	4.38	0.577	0.327	1.0000	1
Local IMF	28	0.10	0.44	4.19	0.545	0.921	1.0000	2
Local PDMF	23	0.17	0.50	2.07	0.700	0.223	1.0000	1
Local PDMF	28	0.12	0.33	2.86	0.600	0.944	1.0000	2
Inner IMF	6	42.30	89.72	1.12	0.811	0.214	0.9946	3
Outer IMF	6	35.90	61.84	1.12	0.897	0.220	0.9944	3
MW spheroid	9	0.15	0.16	1.05	1.00	1.207	0.9908	4
GR 8	6	4.58	5.66	1.23	0.930	1.299	0.8616	5
M33	11	12.76	17.24	1.06	0.976	0.253	1.0000	6
NGC 3031	2	0.78	1.56	1.49	0.843	0.000	1.0000	7
NGC 4258	5	1.71	1.84	1.00	1.000	0.840	0.8398	7
NGC 4594	3	1.13	1.33	0.92	0.998	3.2E − 3	0.9545	7
NGC 5194	3	5.44	9.37	0.29	0.900	9.6E − 5	0.9922	7

REFERENCES.—(1) Miller & Scalo 1979; (2) Basu & Rana 1992; (3) Garmany et al. 1982; (4) Richer & Fahlman 1992; (5) Aparicio et al. 1988; (6) Berkhuijsen 1982; (7) Ellis et al. 1982.

the CIs in both the inner and the outer part of the Galaxy, we find that there seems to be more coagulation occurring in the inner part than in the outer part. We must thus conclude that, on the whole, there is more coagulation in the inner part of the Galaxy but that there is no direct relationship between coagulation and distance from the center.

We also searched for any relationship between the CIs and the distance from the plane of the Galaxy (for *all* the clusters), but we found nothing except maybe that the smallest values of C are found closer to the plane (Fig. 3*a*). A plot of z versus $\bar{m}/m_0$ in Figure 3*b* shows the same tendency: the clusters that have experienced more coagulation are found closer to the plane of the Galaxy. This could be explained by a higher gas density, which lowers the Jeans mass (because $M_J \propto \rho^{-1/2}$), which in turn increases the number density of fragments and the probability of collisions—hence there is more coagulation. But this is only a tendency, not a clear-cut relationship. There could also be some bias because of the fact that we find more open clusters near the plane, and more chance of finding highly "coagulated" clusters. In other words, the standard deviation of the distribution is highest for greater numbers ($\sigma \propto N^{1/2}$) that is, nearer the plane. The fact that the clusters close to the plane have not *necessarily* experienced a high amount of coagulation also supports this explanation.

TABLE 8

GALAXIES: FITS OF THE POWER-LAW MODEL

Name (1)	Γ (2)	σ_y (3)	χ^2 (4)	Probability (5)	Reference (6)
Local IMF	−1.30	0.08	81.40	0.0000	1
Local IMF	−1.39	0.07	6291.06	0.0000	2
Local PDMF	−2.95	0.18	4286.00	0.0000	1
Local PDMF	−2.87	0.15	238001.02	0.0000	2
Inner IMF	−0.39	0.23	3.73	0.4433	3
Outer IMF	−1.11	0.09	0.19	0.9958	3
MW spheroid	−2.95	0.49	246.99	0.0000	4
GR 8	−0.97	0.47	8.41	0.0776	5
M33	−2.82	0.06	2.73	0.9741	6
NGC 3031	−3.63	...	0.00	1.0000	7
NGC 4258	−4.30	0.28	67.04	0.0000	7
NGC 4594	−3.47	0.65	14.30	0.0002	7
NGC 5194	−1.84	0.32	16.92	0.0000	7

REFERENCES.—(1) Miller & Scalo 1979; (2) Basu & Rana 1992; (3) Garmany et al. 1982; (4) Richer & Fahlman 1992; (5) Aparicio et al. (1988); (6) Berkhuijsen 1982; (7) Ellis et al. 1982.

TABLE 9

CORRELATION BETWEEN THE TWO CIs

Type of Stellar Group	r	Number of points
Open cluster	0.799	54
OB association	0.973	16
Globular cluster	0.890	16
Galaxy	0.939	13

TABLE 10

EXTREME VALUES OF C

Type of Stellar Group	Minimum	Maximum	$\langle C \rangle$	σ
Open cluster	0.132	0.999	0.788	0.243
OB Association	0.211	0.936	0.719	0.209
Globular Cluster	0.588	0.996	0.921	0.109
Galaxy	0.545	1.000	0.829	0.169

TABLE 11

EXTREME VALUES OF $\bar{m}/m_0$

Type of Stellar Group	Minimum	Maximum	$\langle \bar{m}/m_0 \rangle$	σ
Open cluster	0.228	86.0	6.33	16.31
OB association	0.935	24.6	3.45	5.84
Globular cluster	0.097	3.46	0.980	0.739
Galaxy	0.29	4.38	1.752	1.281

TABLE 12

MEAN VALUES OF THE PROBABILITY THAT FIT IS GOOD

Type of Stellar Group (1)	⟨Probability⟩ (2)	σ (3)	$\langle \text{Probability} \rangle_\Gamma$ (4)	σ_Γ (5)
Open cluster	0.918	0.139	0.246	0.372
OB association	0.955	0.072	0.299	0.357
Globular cluster	0.998	0.003	0.397	0.436
Galaxy	0.971	0.055	0.269	0.429

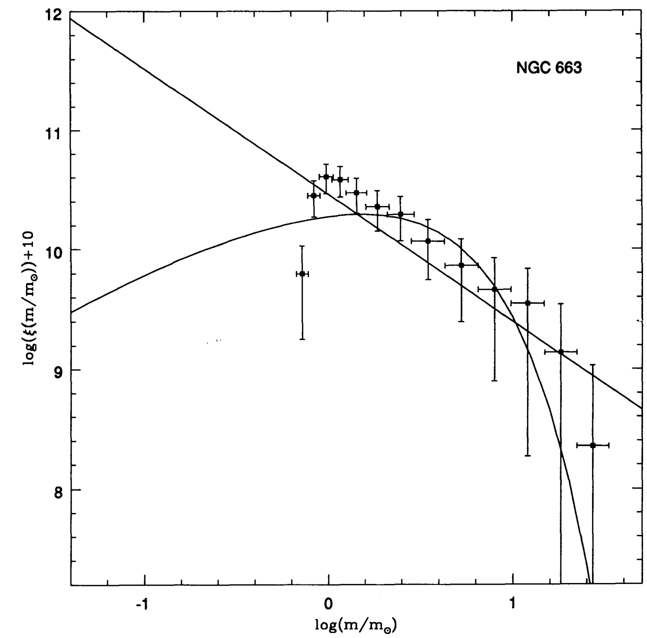

FIG. 1*a*

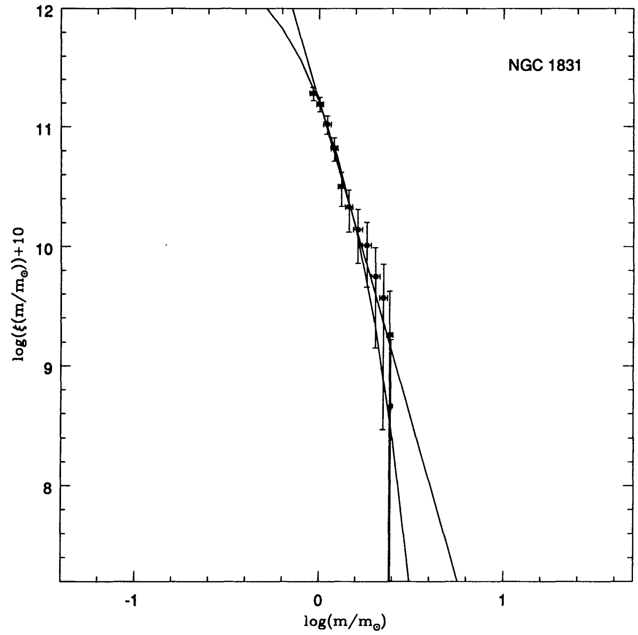

FIG. 1*b*

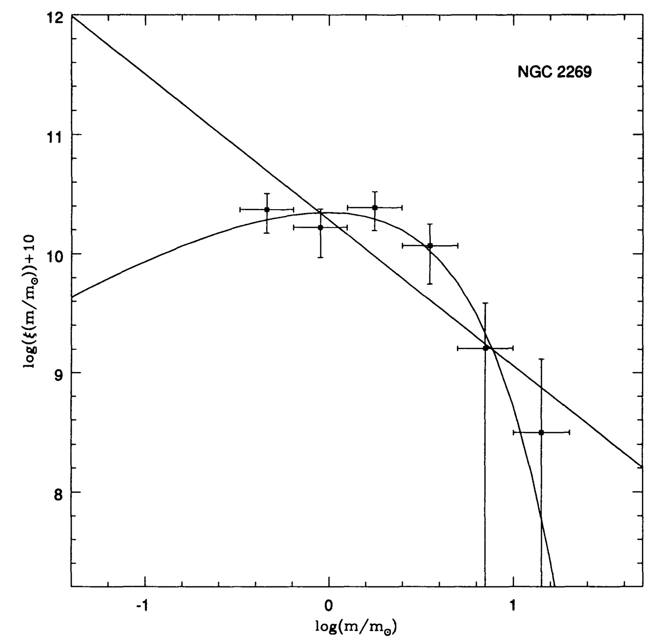

FIG. 1*c*

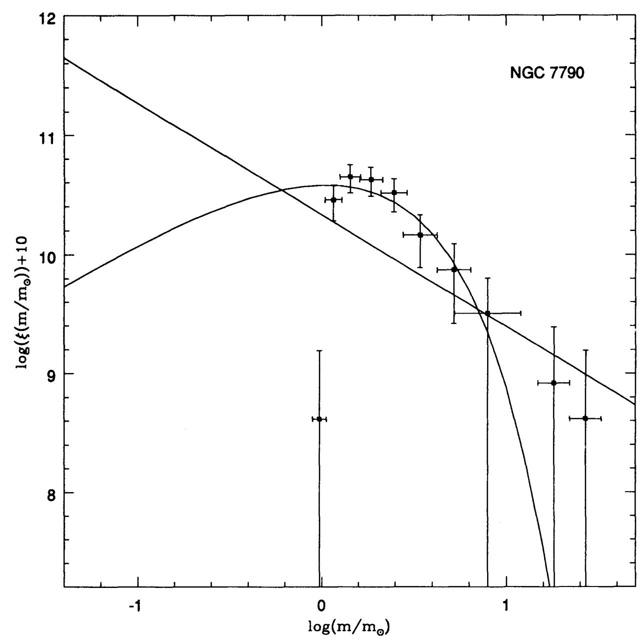

FIG. 1*d*

FIG. 1.—Examples of good fits of mass spectra with the coagulation model. In all cases the solid curve and the solid line represent, respectively, the best-fit coagulation model and the best-fit power-law model for comparison purposes (see text for more details). (*a*) Open cluster NGC 663. Although the high-mass end of the mass spectrum is well fitted, the low-mass end shows that fragmentation is more important in this range. (*b*) Open cluster NGC 1831. (*c*) Open cluster NGC 2269. (*d*) Open cluster NGC 7790. (*e*) Pleiades. (*f*) Globular cluster M5.

So the evidence is as deceiving for this case as for the previous one: we find no clear relationship between the position of an open cluster in the Galaxy (in R or z) and the amount of coagulation that occurred in that cluster.

Some authors have found some indication for a link between the age of a cluster and the slope of its mass function (Tarrab 1982; Francic 1989). We think that there is a danger in comparing spectral indices of different open clusters (and that applies to *any* type of star cluster), since most often these indices are calculated for *different mass intervals*. In order to have a meaningful comparison, one would have to calculate the indices in the same mass interval, which is almost impossible to do if one is to take any large sample of clusters, on account of the large differences in the mass intervals spanned (one has only to look at the large variations in the mean mass of the stars for different clusters in Table 1 to be convinced of this fact). We feel, however, that it is possible to do better with the CIs, since these parameters define the form of the curve and

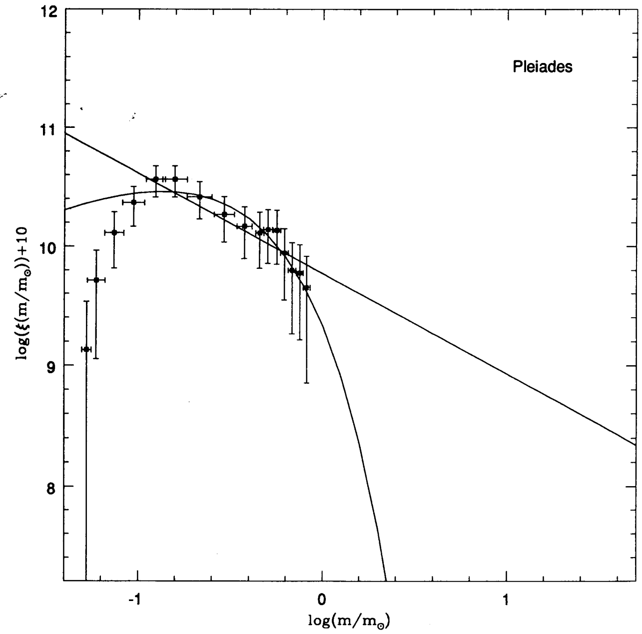

FIG. 1*e*

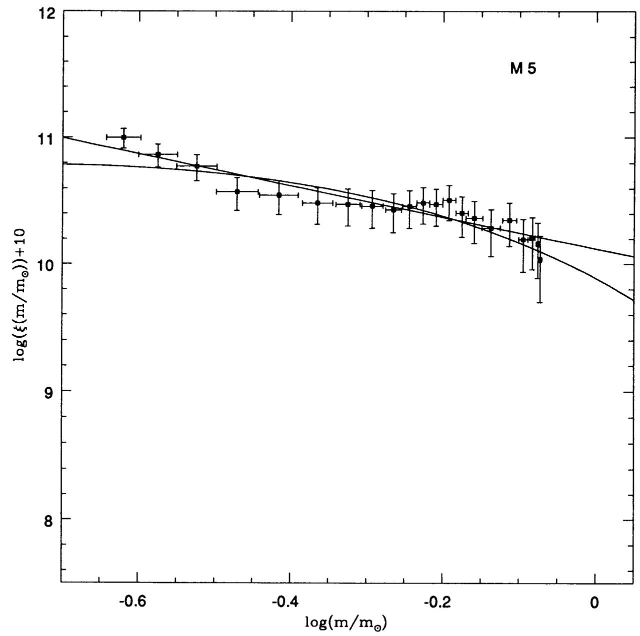

FIG. 1*f*

are independent of the mass interval at which they are calculated, as long as incompleteness is not too important at the low-mass end of the spectrum. In any case, the problem of incompleteness also affects power-law fits.

We therefore searched for any link between C and $\bar{m}/m_0$ and the age of the cluster. Again, no relationship is found (see Table 13). It is possible that there is a selection effect because our sample covers the span 2×10^6 to 6×10^9 yr. In other words, the amount of coagulation could depend on the age of the cluster if $t \lesssim 10^7$ yr, and then reach a constant value for later times. This behavior would be explained by the fact that most clusters have relaxation times (Spitzer & Hart 1971) of the order of 10^6 yr, so the probability of collision and, consequently, the probability of coagulation are higher before the cluster has settled. Because it is difficult to measure accurately the age of very young clusters (and because we only have two clusters whose age is lower than 10^7 yr), we will have to wait for new techniques and new data to verify this hypothesis.

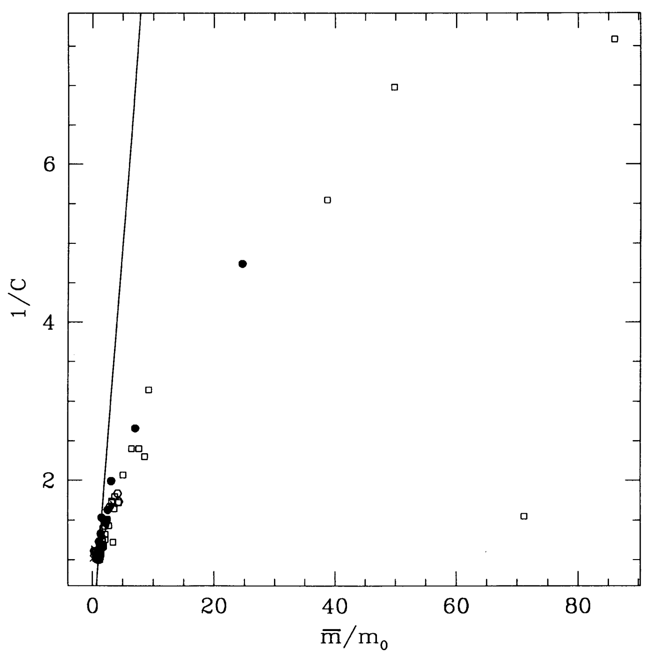

FIG. 2*a*

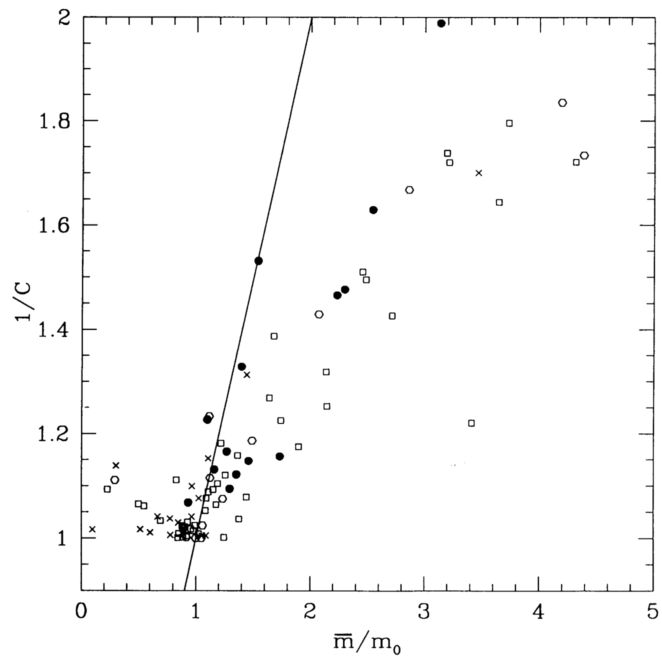

FIG. 2*b*

FIG. 2.—Relationship between $1/C$ and $\bar{m}/m_0$, where we have included all the data from Tables 1–4 (*open squares*: open clusters; *filled circles*: OB associations; *crosses*: globular clusters; *open hexagons*: galaxies). In (*b*) is shown a blowup of the crowded part of (*a*). In both cases the solid line represents the expected relationship if no mass loss has occurred in all the groups. As can be seen, mass loss has indeed occurred in virtually all the cases.

TABLE 13

CORRELATION COEFFICIENTS: OPEN CLUSTERS

Parameter	r(C)	$(\bar{m}/m_0)$	Number of Points
R	−0.221	0.162	34
R (young)	0.837	0.062	7
z	0.229	−0.191	34
Diameter	0.045	−0.028	34
Density	0.037	−0.117	34
$\bar{m}$	−0.116	0.018	57
[Fe/H]	−0.473	0.427	11
Turnoff	0.300	−0.329	34
log (age)	0.311	−0.328	38
Total M_V	−0.222	0.198	35
Spectrum	0.309	−0.299	32
Richness	−0.098	0.103	34
Trumpler concentration	0.109	−0.081	37
Trumpler range	0.016	−0.011	37
Trumpler richness	0.015	0.018	37
$B-V$	0.258	−0.230	33

NOTE.—From top to bottom: distance from the center of the Galaxy, same but for clusters with log (age) < 7, distance from the plane of the Galaxy, diameter of the cluster, mass density of the cluster, mean stellar mass, integrated metallicity, turnoff point, logarithm of the age of the cluster, total visual absolute magnitude, spectral type of the brightest star in the cluster, richness class, Trumpler concentration class, Trumpler range in brightness class, Trumpler richness class, color excess in the *UBV* system.

We did find one interesting possible correlation between the CIs and the metallicity [Fe/H]. Indeed, the clusters that have the highest value of coagulation (the smaller C or higher $\bar{m}/m_0$) also have the highest value of [Fe/H] (see Fig. 4). On the other hand, a Pearson r-coefficient correlation analysis does not support this finding, since the r-coefficient (see Table 13) for each CI is not so large. Still, the fact that both CIs show the same tendency merits more attention.

There are two ways to explain the tendency toward higher metallicities for higher coagulation (if indeed this tendency is not due to a random fluctuation). First, suppose that the metallicity we measure today is a direct consequence of what it was at the formation of the star cluster. Let us consider the Jeans radius (Jeans 1928):

$$R_J = k \frac{GM}{R_g(T/\mu)}, \tag{13}$$

where k is a constant that depends on the boundary conditions, R_g is the gas constant, G is the gravitational constant, and T and μ are the temperature and mean molecular weight in the cloud. Since we are more interested in the behavior than in the exact value of the parameters, we can write

$$R_J \propto \frac{M}{T}, \tag{14}$$

where we suppose that the mean molecular weight is constant throughout the cloud.

We know that the effect of a higher metallicity is to cool a cloud faster. We can now investigate the effect of a smaller temperature on the value of M_J and R_J, since the cross section of a fragment will affect the coagulation rate. Suppose for now

TABLE 14

CORRELATION COEFFICIENTS: OB ASSOCIATIONS

Parameter	r(C)	$r(\bar{m}/m_0)$	Number of Points
Diameter	0.261	−0.268	5
$\bar{m}$	−0.305	0.243	16
Number of members	0.387	−0.455	5
Spectrum	0.226	−0.383	6

NOTE.—From top to bottom: diameter of the association, mean stellar mass, number of members of the association, spectral type of the brightest star.

TABLE 15

CORRELATION COEFFICIENTS: GLOBULAR CLUSTERS

Parameter	r(C)	$r(\bar{m}/m_0)$	Number of Points	Source
log R	0.001	0.211	16	1
log z	0.124	0.036	16	1
$\bar{m}$	0.396	−0.600	16	
log r_c	0.299	−0.168	16	1
log r_h	0.381	−0.213	16	1
log ρ_0	−0.296	0.258	16	1
log $t(r_c)$	0.282	−0.112	16	1
log $[t(r_h)]$	0.318	−0.097	16	1
σ_v	0.042	0.150	16	2
log $[\rho_0(m)]$	−0.188	0.182	16	2
r_s	0.344	−0.232	16	2
M/L_v	0.305	−0.397	16	2
M/L_v central	0.149	−0.220	16	2
log M	−0.085	0.263	16	2
[Fe/H]	−0.212	0.076	16	1
Zr/Fe	0.069	0.994	3	3
Ba/Fe	−0.358	0.997	4	3
Eu/Fe	−0.957	0.116	3	3
La/Zr	0.511	−0.755	3	3
Si/Fe	−0.263	0.803	5	3
Ca/Fe	0.159	0.515	4	3
Ti/Fe	0.450	−0.472	5	3
Concentration	−0.262	0.286	16	2
Total M_V	0.010	−0.199	16	1
$B-V$	−0.031	−0.227	16	2

NOTE.—From top to bottom: logarithm of the distance to the center of the Galaxy, logarithm of the distance to the plane of the Galaxy, mean stellar mass, logarithm of the core radius, logarithm of the half-light radius, logarithm of the central luminosity density in the V band, logarithm of the central two-body relaxation time, logarithm of the half-light relaxation time, velocity dispersion, logarithm of the central mass density, scale radius, global mass-to-light ratio, central mass-to-light ratio, logarithm of the total mass of the cluster, metallicity indexes, total absolute visual magnitude, color excess.

SOURCES.—(1) Djorgovski 1993; (2) Pryor & Meylan 1993; (3) Brown et al. 1991.

TABLE 16

CORRELATION COEFFICIENTS: GALAXIES

Parameter	r(C)	$r(\bar{m}/m_0)$	Number of Points
Hubble type	−0.448	0.300	12
Total M_V	0.088	−0.124	12
Diameter	−0.618	0.562	12
$\bar{m}$	0.144	−0.282	14
log (mass)	−0.119	0.108	12
$B-V$	−0.060	0.099	6

NOTE.—From top to bottom: Hubble type of the galaxy, total absolute visual magnitude, diameter of the galaxy, mean stellar mass, logarithm of the total mass of the galaxy.

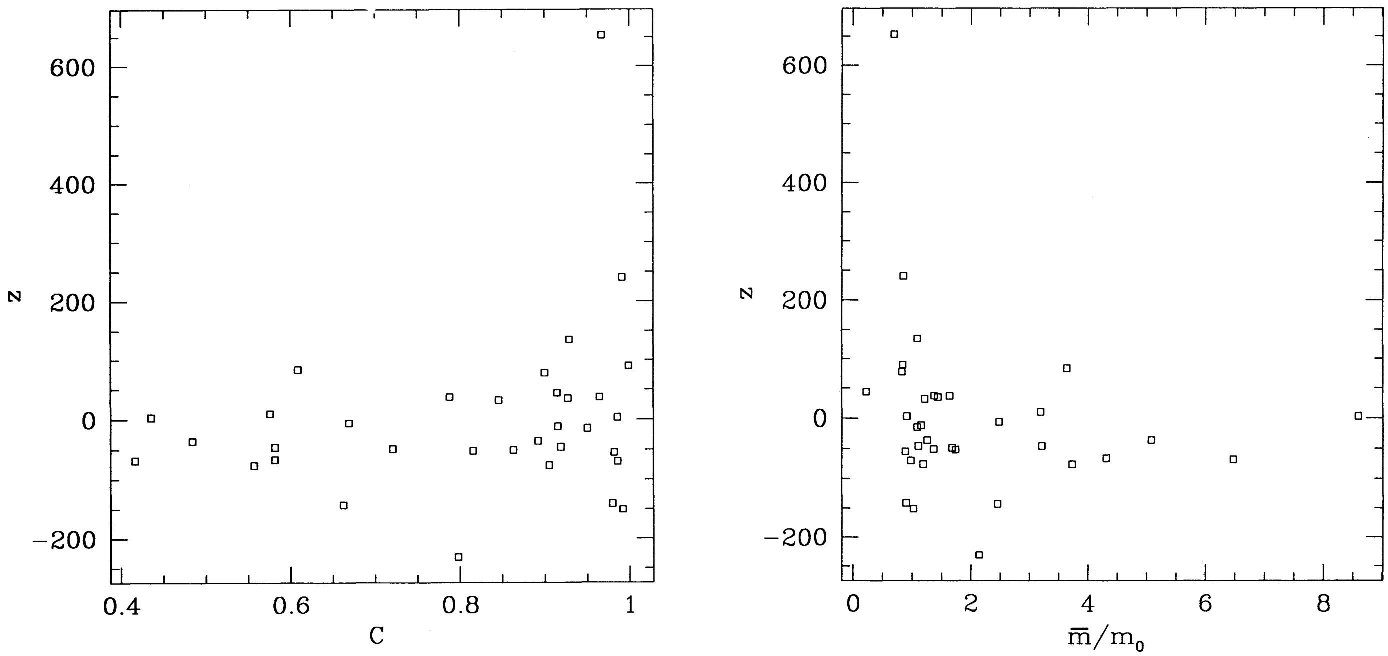

FIG. 3*a* FIG. 3*b*

FIG. 3.—(*a*) Plot of *C* vs. the distance from the open cluster to the plane of the Galaxy. The clusters that have experienced the most coagulation are found closer to the plane (see § 4.1 for more details). (*b*) Same as (*a*), but for $\bar{m}/m_0$. Again, no clear relationship is found.

that *M* is constant; then a lower temperature will raise the value of R_J, hence the fragment's cross section and the probability of a collision. Thus, for a constant mass, higher metallicity in a cloud can raise the amount of coagulation.

Now suppose we vary *M* instead of R_J; a lower temperature will then mean a lower Jeans mass. Suppose that we have a cloud of mass M_c and radius R_c; if we divide the cloud into M_c/M_J fragments,[4] we expect to have a higher number density of fragments and, hence, a higher probability of collisions. Thus, for a constant radius, a higher metallicity in a cloud will also raise the amount of coagulation.

[4] We assume that the fragmentation takes place in a very short time at the formation of the cluster and stops afterward.

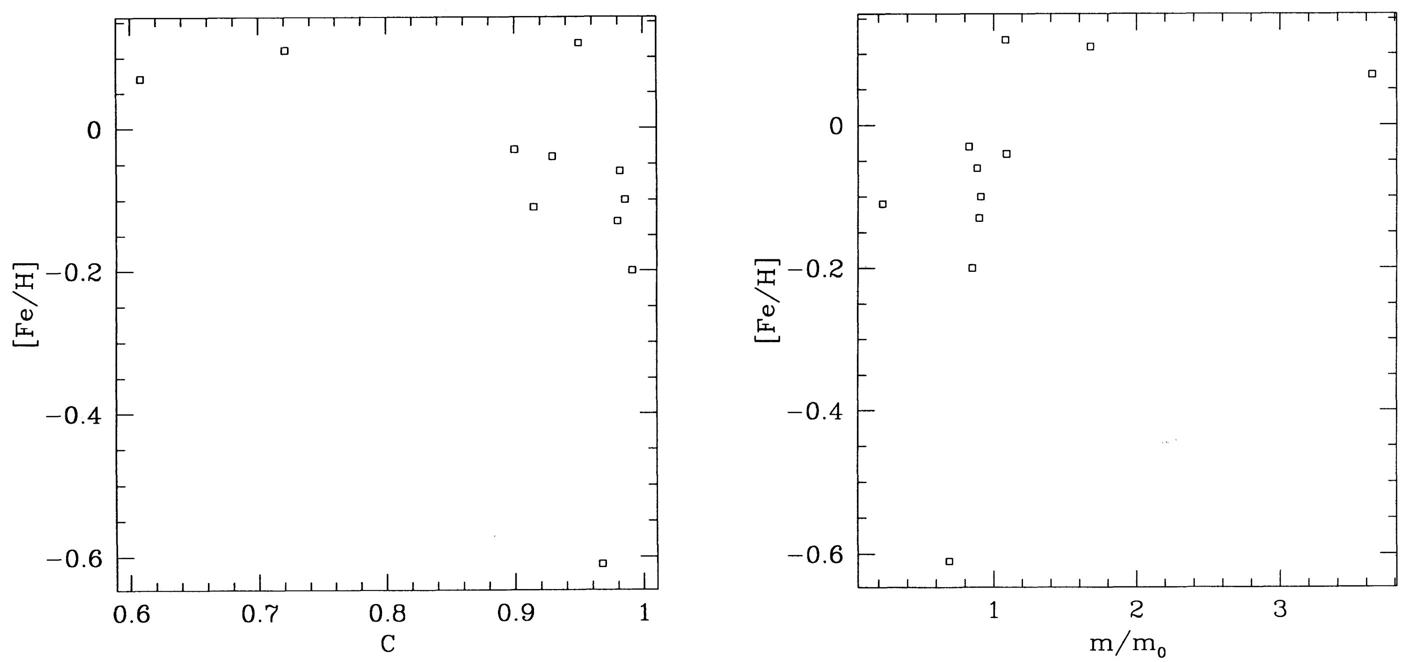

FIG. 4*a* FIG. 4*b*

FIG. 4.—(*a*) Possible correlation between the coagulation indicators and the metallicity of open clusters, (*a*) for *C* and (*b*) for $\bar{m}/m_0$. Whether the metallicity is a consequence of coagulation or vice versa is not clear.

The other way to explain the correlation between metallicity and the amount of coagulation is to assume that [Fe/H] is a *consequence* of coagulation. If higher mass stars are formed by collisions, we then expect that metals will be formed earlier and in larger amounts in a cluster with massive stars than in a cluster which has fewer massive stars. It then follows that a higher amount of coagulation can produce open clusters with higher metallicities, as suggested by Figure 4.

Finally, no link was found between the CIs and the total integrated absolute magnitude of the cluster, its linear diameter, its density, the mean mass of its stars, its turnoff point, its Trumpler type, its integrated $B-V$ or the spectral type of its brightest star (see Table 13). The number of clusters was in most cases high enough to make reliable estimates of the Pearson correlation factor.

4.2. *OB Associations*

Because OB associations are loosely bound and have a relatively small number of stars, it is difficult to study them in any accurate manner. In order to find any correlations, we have to know the characteristics of each of these stellar groups, and, unfortunately, not much has been done in this area. The best source of information on the physical characteristics of OB associations is Reprecht, Balasz, & White (1981a).

As for the case of open clusters, we find no correlation between the linear diameters of the association and the two CIs, supporting again the universality of the coagulation process. Moreover, there is no connection between the number of stars (which is quite uncertain), the mean mass of these stars, or the earliest spectral type of these and either C or $\bar{m}/m_0$. We must, however, stress the fact that the number of associations studied in this paper is still relatively too small to allow any solid conclusions. We have, counting the Orion subgroups as one group, 12 different OB associations in our paper. So nothing much can be said about coagulation in OB associations, except that it seems to be occurring just as in the other types of stellar groups that we have studied in this paper.

4.3. *Globular Clusters*

We consulted the catalogs by Brown, Burkert, & Truran (1991), Pryor & Meylan (1993), and Djorgovski (1993) for the data on the physical characteristics of the clusters in our sample. The results are shown in Table 15. The parameters used in the correlation search are, from top to bottom, distance to the Galactic center, distance to the Galactic plane, mean mass of the stars, core radius, half-light radius, central luminosity density in solar V-band units, central two-body relaxation time, median two-body relaxation time, velocity dispersion, central mass-density, scale radius, global mass-to-light ratio, central mass-to-light ratio, cluster mass, metallicity, Zr/Fe, Ba/Fe, Eu/Fe, La/Zr, Si/Fe, Ca/Fe, Ti/Fe, concentration, total absolute magnitude in the V-band, and $B-V$.

Following the apparent connection between the CIs and the metallicity that we found for open clusters, we looked for the same relationship in globular clusters. Obviously, because the stars making up the globular clusters are of Population II, the metallicity of the cluster will always be negative, and we will not be able to make comparisons in the same metallicity range, as we did for open clusters. But we can look for a similar tendency, that is, the higher the metallicity of the cluster, the higher the corresponding coagulation will be. As can be seen in Figure 5, no relationship between [Fe/H] and the CIs is found. Moreover, the Pearson r-coefficients for this case are very small.

We looked also at the possibility of correlations between [Si/Fe], [Ba/Fe], [Ti/Fe] and the CIs. The Pearson coefficients were large for some of them (0.997 for [Ba/Fe] and $\bar{m}/m_0$) but the number of points used for the calculations is

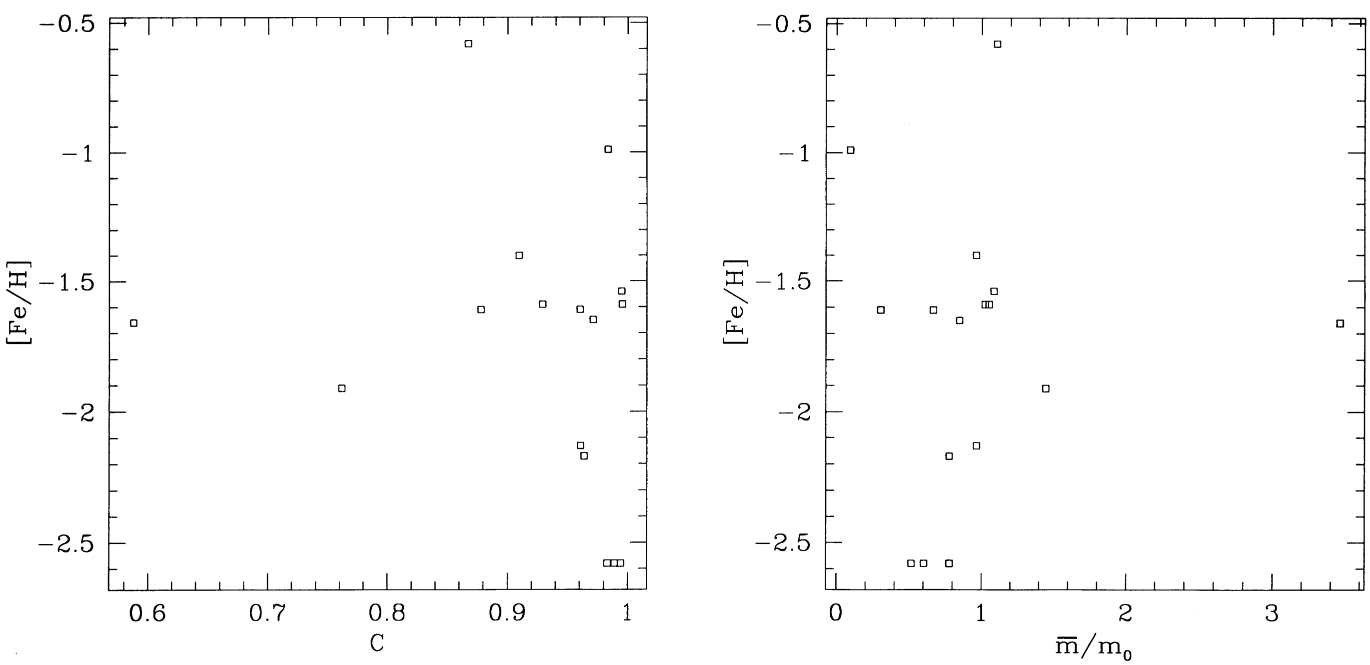

FIG. 5*a* FIG. 5*b*

FIG. 5—(*a*) [Fe/H] vs. C for globular clusters. (*b*) [Fe/H] vs. $\bar{m}/m_0$ for globular clusters. Neither figure shows a relationship between the amount of coagulation and the metallicity.

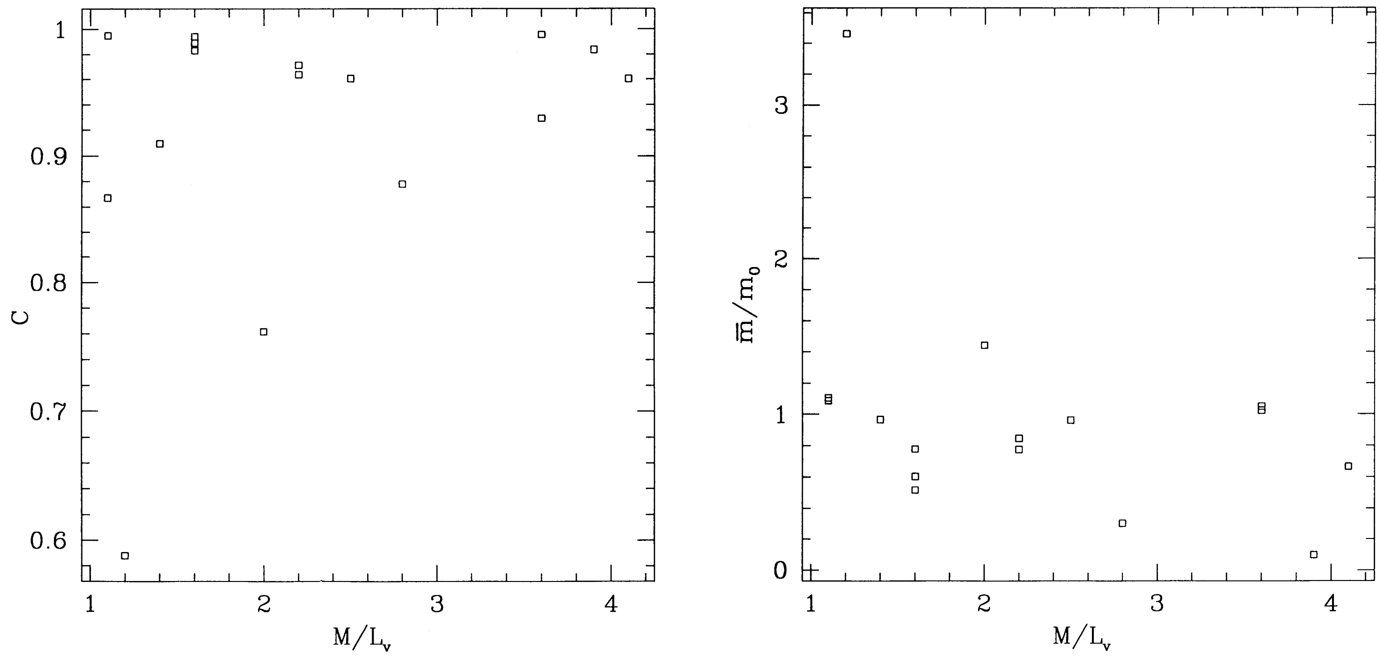

FIG. 6a FIG. 6b

FIG. 6.—No relationship is found between the CIs and the M/L_v ratio. (a) C vs. M/L_v; (b) $\bar{m}/m_0$ vs. M/L_v.

too small to allow any valid conclusions to be drawn. Furthermore, the CIs did not agree with each other. We thus feel that one should not read any more into this than a chance configuration.

One cannot say the same for M/L_v. Indeed (see Fig. 6), it seems that the more coagulation there is, the smaller the M/L_v ratio is. It is not a one-to-one relationship (hence the relatively small Pearson coefficients), but, as for the metallicity in open clusters, the globular clusters with the most coagulation also have the smallest M/L_v. This could be explained by the fact that coagulation takes fragments that otherwise would have been too small to become stars and puts them together to make one actual star, therefore reducing the amount of low-luminosity mass and, consequently, reducing M/L_v. It is disquieting, though, that this tendency does not hold for the central value of M/L_v (see Fig. 7), where the center of the

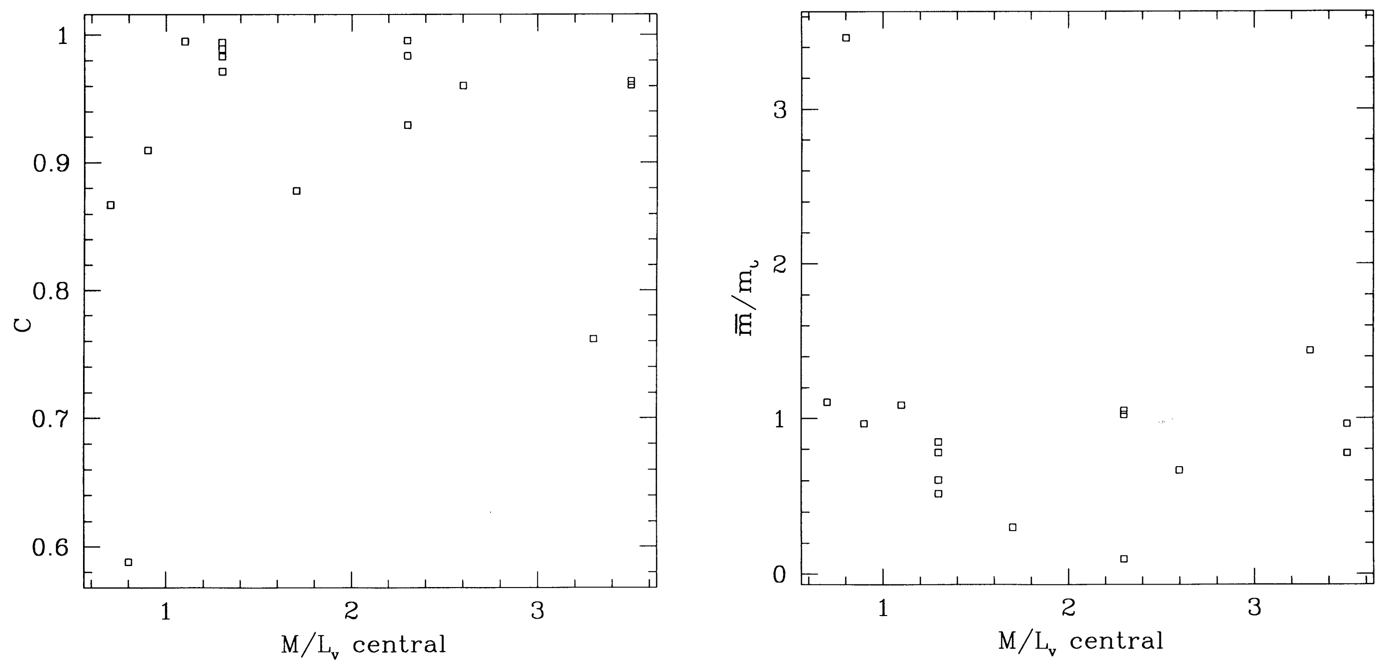

FIG. 7a FIG. 7b

FIG. 7.—Same as Fig. 6, but for the central value of M/L_v

globular cluster is supposed to be where the most coagulation occurred. In fact, if one is to take out the point with $\bar{m}/m_0 \approx 3.5$, then one gets a scattering of points. Much the same happens for C if one is to forget the two points of lowest value. It would be interesting to look at the M/L_v of open clusters to find out whether they show a similar behavior. Unfortunately, it is not feasible because, on the one hand, we do not have those data and, on the other, those data are (even for globular clusters) relatively imprecise. We thus conclude that the data do not show a convincing relationship between the CIs and the M/L_v ratio.

As for the other quantities (distance to the Galactic center, distance to the Galactic plane, mean mass of the stars, core radius, half-light radius, central luminosity density in solar V-band units, central two-body relaxation time, median two-body relaxation time, velocity dispersion, central mass-density, scale radius, cluster mass, Zr/Fe, Eu/Fe, La/Zr, Ca/Fe, concentration, total absolute magnitude in the V-band, and $B-V$), there does not seem to be any correlation between these and the CIs.

4.4. *Galaxies*

The IMF data for galaxies other than our own and M33 is quite uncertain because it is unfortunately practically impossible to obtain a *direct* measurement of their IMF; one has to rely on other techniques (see Scalo 1986 for a review of these techniques). We must also point out that, apart from the intrinsic uncertainty of the data, the number of points is very small for any judgement on the goodness of fit of any model. (It is obvious that one can fit *any* curve to three data points). So the best-fit values for NGC 3031, NGC 4258, NGC 4594, and NGC 5194 must be taken as indicative only. As for the others, the number of data points is quite sufficient for our purpose.

It is important to note that in comparing mass spectra of different galaxies, one is comparing spectra made up of different types of stellar associations (open clusters, OB associations, globular clusters). Hence, these mass spectra will depend strongly on their "ingredients." Except for our Galaxy, the mass spectra of different galaxies are the result of different evolutions.

Furthermore, it is not clear how much the field star IMF is influenced by escaped stars from open clusters and OB associations. In other words, one is looking at some kind of mean of the different processes by which stars are formed. We must thus look at the following results with these factors in mind.

The six physical characteristics of a galaxy that we felt could be connected in some way to coagulation are its Hubble type, its absolute magnitude, its linear diameter, the mean mass of its stars, its total mass, and its $B-V$. Table 16 presents the results from the correlation search.

From the value of the Pearson coefficients for the Hubble type and the diameter of the galaxy, one might be tempted to say that there is a correlation between these parameters and coagulation. We looked into this (Figs 8 and 9) and although it seems that the largest amount of coagulation is found in late-type spirals, we must point out that we only have three data points that are not Sc spirals out of a total of 12 points. In other words, the variety of galaxy types in our study is too small to enable us to draw any strong conclusions. One has only to look at the spread of values for Sc galaxies in Figure 8 to be convinced of this fact.

Concerning the apparent connection between the diameter of a galaxy and the importance of coagulation in it, there is a tendency toward more coagulation for bigger diameters. Again, as for the Hubble type, the diversity of diameters and the number of points is too small to make any valid conclusions.

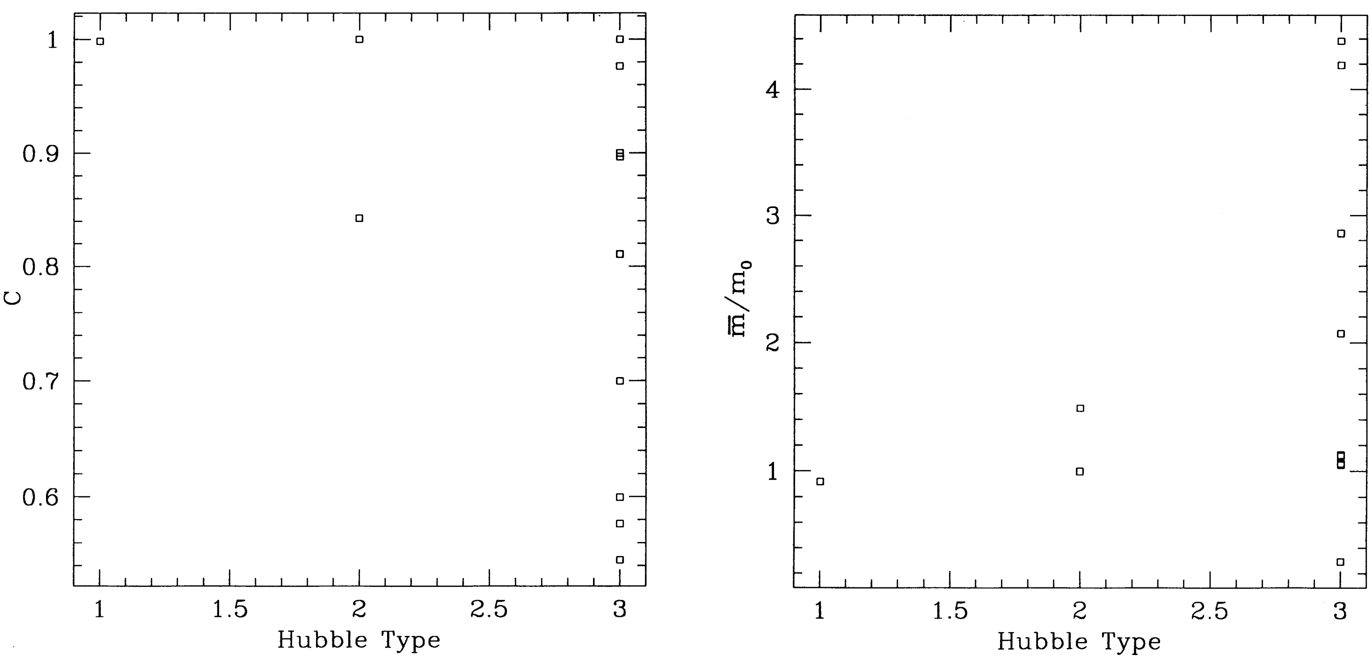

FIG. 8a FIG. 8b

FIG. 8.—Apparent relationship between the Hubble type of a galaxy and the amount of coagulation that occurred. (*a*) Hubble type vs. C; (*b*) Hubble type vs. $\bar{m}/m_0$.

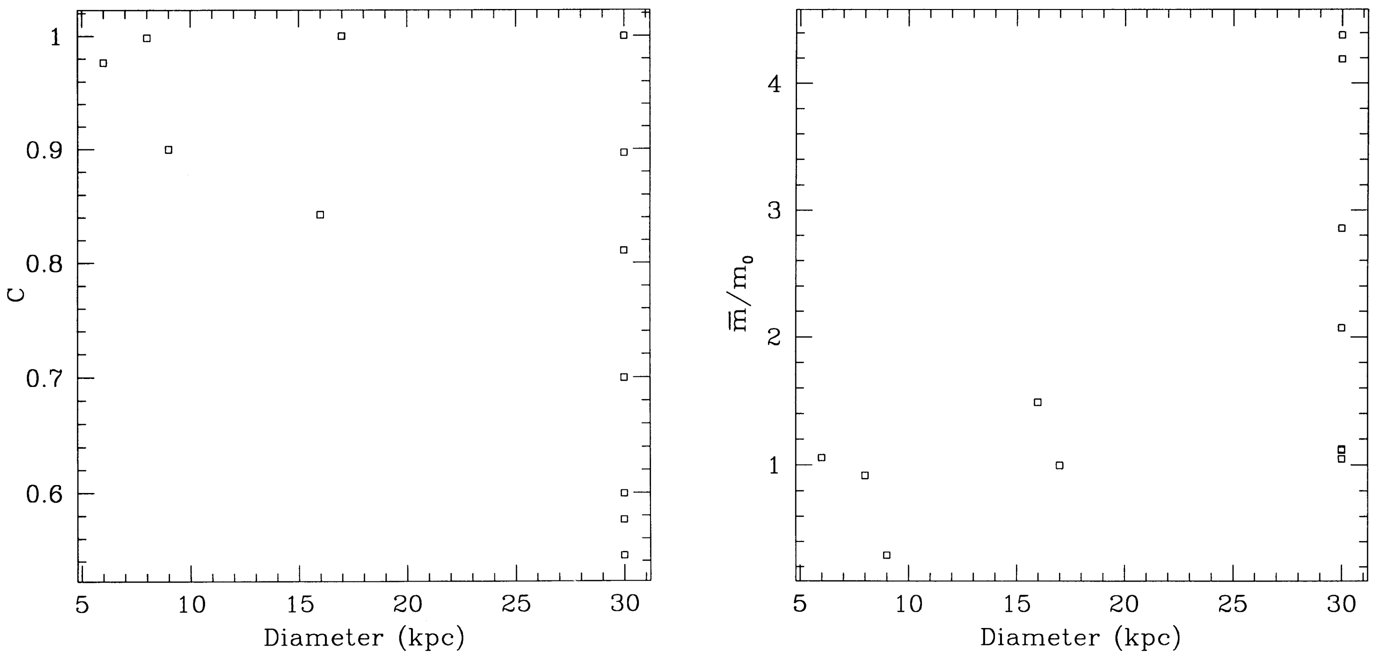

FIG. 9a FIG. 9b

FIG. 9.—Apparent relationship between the diameter of a galaxy and coagulation. (*a*) Diameter vs. C; (*b*) diameter vs. $\bar{m}/m_0$.

It was found, however, that there is more coagulation in the central regions of the Galaxy than in the outer regions, in agreement with what we found for the open clusters in § 4.1. This could be explained by the higher star densities found in the center, which raise the probability of collisions for the same reason stated earlier about the Jeans mass. If this effect is real, then we will have to remember to take it into account when comparing the Galaxy's IMF with the IMF of other galaxies.

No other correlation was found between physical properties of galaxies and the CIs. Variations are found, but none that are systematic. Again, the small number of galaxy IMFs studied in this paper, along with the uncertainty of the data, might preclude our finding any existing relationship between the amount of coagulation and the properties of the galaxy.

5. DISCUSSION

What can we conclude from the probability of fit results? First, that in some cases the coagulation model is very good (see Fig. 1) at reproducing the mass spectrum, probably because fragmentation was negligible compared with coagulation. However, this conclusion must be shaded by the fact that some mass loss must have occurred in the relaxation of the cluster. The effect of evaporation would be to eject preferentially the less massive stars and exaggerate the contribution of the more massive stars, mimicking coagulation. Judging from Figure 2, the evaporation of stars has most certainly occurred. Still, as expected (Bastien 1981), the coagulation model fits the high-mass end very well. Even in the cases where the *total* fit is not perfect, the high-mass end of the mass spectrum is well fitted. Fragmentation-only models presumably do not reproduce this part of the spectrum adequately. In any case, fits obtained with the coagulation model are much better than those obtained with a power law.

The second conclusion is, obviously, that the coagulation model does not appropriately represent reality in some (25% have a probability of good fit lower than 95%) of the cases. Again, mass loss (of a different kind) could be responsible for some of them. Indeed, mass loss by stellar winds would diminish the total mass of the cluster but not the total number of stars, making the low-mass stars more important than the more massive stars in numbers. This would have the same effect as making coagulation less important compared with fragmentation. Still, 84.5% have a probability of good fit of more than 90%, which is surprising in view of the preceding facts. In other words, the pure coagulation model gives a very good representation of reality, especially in the high-mass range, even though it has only two adjustable parameters. We feel that its simplicity is a great advantage of this model.

How are we to separate the effects of mass loss of the cluster from the effects of fragmentation and coagulation? One possibility is the "mass-loss indicator" that we described in § 2.1. Certainly this indicator lets us know the amount of mass loss by the cluster without knowing specifically the physical processes involved, be it mass loss by evaporation, by stellar winds, or by some other process. But we must remember that this indicator is valid *only in the context of pure coagulation*, which we know is not exactly the case. The only cases when the pure coagulation model will work is when fragmentation either does not occur any more or is negligible compared with coagulation. So the mass-loss indicator will also, by extension, work only in this instance.

We are then left with the same problem. One way to avoid or minimize the mass-loss problem would be to take young clusters, that is clusters whose age is smaller than their relaxation time. The relaxation time for a typical cluster is, as stated in § 4.1, of the order of 10^6 yr. Unfortunately, because of high absorption in the visible range for young clusters, it is difficult to obtain good luminosity functions. One way to circumvent this is to make observations in the infrared region of the spectrum. Some authors (Wilner & Lada 1991; Lada, Bally, & Stark 1991a; Lada et al. 1991b, c; Straw et al. 1987) have already done so. The main problem resides in transforming the luminosity function into a mass spectrum. Indeed, most of these stars are not yet on the main sequence, and the mass-luminosity function for young stars is also quite uncertain. Thus, a lot of theoretical work is still needed to resolve this problem (see, for example, Palla & Stahler 1993).

Another assumption of the model that could be arguable lies in our supposition that all collisions are purely nonelastic and that no disruption occurs. A paper by Habe & Ohta (1992) investigates the gravitational instability induced by a cloud-cloud collision and concludes that there may be some disruption of the clouds upon collision. In other words, the mass M of a cloud formed by the collision of clouds of masses m_1 and m_2 is not necessarily equal to $m_1 + m_2$. It is not clear that all the matter ejected by the collision will be accreted by the resulting cloud. A more realistic treatment of this problem would be to include dynamical fragmentation, i.e., fragmentation resulting from the collision of two fragments (as opposed to gravitational fragmentation, which is what we mean by fragmentation in the rest of this paper) in calculating the resulting mass spectrum. But that is outside the scope of this paper.

The coagulation model is also better at fitting data than the much-used power-law fit in which one assumes that the data follow equation (12). One has only to look at Table 12 to be convinced of this fact. One could certainly fit a Gaussian curve to the data as easily and with the same number of free parameters. But the coagulation model has the advantage of coming from *physical* assumptions, whereas the Gaussian model is simply a probabilistic model. In this sense, we feel that the coagulation model, in spite of its shortcomings, is an improvement over the other models.

It is a well-known problem that the power-law model implies a physically unrealistically large number of small-mass fragments. It is more probable that there is a so-called *turnover* of the mass spectrum. This turnover has been observed in some open clusters (in the Pleiades, for example), and the question is whether it is real or is simply an observational artifact. Indeed, there is a limiting absolute magnitude that is reached in the observation of a star cluster; this magnitude limit makes it impossible to observe stars whose mass is below the mass limit corresponding to the magnitude limit. This effect is not clear-cut, so it could make the mass spectrum *bend* in the low-mass end. Moreover, clusters that are too far will obviously not show this turnover if it happens in an observationally forbidden mass region. So observations tell us that certain open clusters show a turnover whereas some others do not; but they cannot tell us whether it happens in *every* cluster. Moreover, one cannot say yet whether the observed turnovers come from mass segregation (i.e., by evaporation of the low-mass stars), from formation processes (fragmentation or coagulation, for example) or from simple incompleteness in the data due to the magnitude-limit effect explained above.

The coagulation model predicts that there should be a turnover in every cluster, regardless of its type. The model is also very flexible in the sense that the turnover can be fitted in any mass range. Moreover, in all the mass spectra where there is a sufficiently large number of reliable points, the curve is indeed a curve and not a straight line. So we think that the Lejeune & Bastien model, although it is an approximation, is better suited to reproducing varied mass spectra than the power-law model if one assumes that the turnover is real.

Another advantage of the coagulation model is that it provides an explanation for the presence of the so-called blue stragglers in some globular clusters (see Leonard 1989 and Fusi Pecci et al. 1992 for reviews of the subject). This type of star was first noticed by Sandage in M3 (Sandage 1953) and has at least three possible explanations. The first is that these stars are in fact binaries whose extended main-sequence (MS) lifetime is due to mass transfer between them. The second is that these stars are single stars which have had some internal mixing and, consequently, an extended MS lifetime compared with other "normal" stars. The third possible explanation is that there have been some inelastic collisions between stars resulting in internal mixing of the two stars' fusion fuel and, again, an extended MS lifetime. Because of the high star densities in the core and the long ages of globular clusters, it is very likely that star collisions are responsible for the existence of most blue stragglers. Recent observations of 47 Tucanae with the *Hubble Space Telescope* add some weight to this explanation. Indeed, Paresce et al. (1991) have observed a high density of blue stragglers in the core of this globular cluster, along with a negative gradient toward the periphery of the cluster. The relaxation time of 47 Tuc being of the order of 10^{-4} times its age (Meylan 1989; Hesser et al. 1987), mass segregation by two-body relaxation has surely taken place, leaving the most massive stars in the core. It is then believed that blue stragglers are either binaries or more massive stars. Moreover, the presence of high-velocity stars in the core found by Meylan, Dubath, & Mayor (1991) supports the idea of close encounters between stars and thus the possibility of collisions. It is interesting to note that all the globular clusters studied in this paper have been extremely well fitted by the model (the mean value of the probability of the fit is 0.998 with a σ of 0.003). Of these 13, six (M3, M71, NGC 5053, NGC 6171, NGC 6397, and ω Cen) have established blue stragglers in their cores (see Fusi Pecci et al. 1992 for all of them; Ferraro et al. 1993 for M3; and Aurière, Ortolani, & Lauzeral 1990 for NGC 6397).

Although Paresce et al. (1991) point out that they cannot yet distinguish observationally between the three possible explanations for the existence of blue stragglers, the coagulation model is certainly not ruled out. As they also point out, more observations of the time variability and spectra of these stars are needed to resolve this problem.

In light of the preceding facts, we feel that, although the coagulation-only model does not explain all the observations, it provides an important contribution for explaining the mass spectra. One must remember that the coagulation-only model is an idealization of what is actually occurring. The model we have treated in this paper assumes that fragmentation took place during a very small time interval at the formation of the cluster and stopped afterward. The mass spectrum resulting from this fragmentation was then assumed to be that of a Dirac delta function, that is, with all the fragments having the same mass initially. Only after fragmentation has stopped can coagulation begin in this model. Another approximation of the coagulation model of Lejeune & Bastien (1986) is that the coagulation rate depends on the sum of the masses. A more appropriate dependence would be m^λ, where λ is in the range $2/3 \leq \lambda \leq 4/3$ as considered by Silk & Takahashi (1979). However, there is no analytic solution with such a coagulation rate, even without taking into account the time dependence.

In reality, of course, the situation is much more complex. First, fragmentation and coagulation must, at least during some time interval, be occurring concurrently. Second, these two processes must vary in time, fragmentation being more important than coagulation at the beginning and vice versa afterward. The logical but cumbersome treatment of the problem would be to resolve the full integrodifferential equation of fragmentation-coagulation by including the time variation.

6. SUMMARY AND CONCLUSION

Starting with the results of Lejeune & Bastien (1986), we tried to assess where and when coagulation could play an important role. We defined two coagulation indicators: C, the ratio of the initial number of fragments to the present one, and $\bar{m}/m_0$, the ratio of the present mean mass of the fragments to the initial one. The coagulation indicators are found from fitting equation (5) to the observed mass functions. Using these two coagulation indicators, we looked for possible links between the amount of coagulation that occurred and the physical traits of the objects studied. One general finding of the present study is that the simple coagulation model as given by equation (2) or equation (5) is better at fitting the observations than the usual power law used so far by many others.

We found that, for open clusters, the only probable link present was with the metallicity of the cluster. On the other hand, the concentration and richness classes, the position in the Galaxy, the linear diameter, the total absolute visual magnitude, the mass density, the mean mass of the stars, the turnoff point, the $B-V$ value, along with the age of the open cluster, were found to have no detectable effects on the importance of coagulation. However, only a small fraction of the clusters studied can be considered as young, i.e., with an age $\lesssim 10^7$ yr.

For the case of OB associations, no relationship was found between the CIs and the linear diameter, the number of stars in the association, the mean mass of the stars or the spectrum of the earliest stars. Much the same can be said about globular clusters: the position in the Galaxy, the mean mass of the stars, the core radius, the half-light radius, the central luminosity density, the central and median two-body relaxation time, the velocity dispersion, the central mass density, the scale radius, the central and global M/L_v ratio, the total mass, the concentration, the total M_v, the spectral type, the $B-V$ value, Zr/Fe, Ba/Fe, Eu/Fe, La/Zr, Si/Fe, Ca/Fe, or Ti/Fe did not seem to affect the occurrence of coagulation. The possible link between metallicity and coagulation found for open clusters could not be assessed with certainty in this type of stellar cluster.

As for galaxies, the quality of the data was not high enough to allow firm conclusions, except for our own Galaxy. There seems to be more coagulation in the center of the Galaxy than toward the outer regions, which is expected because of the higher densities found in the center that, in turn, make the probability of collisions higher. No correlation was found between the Hubble type, the linear diameter, the absolute integrated magnitude, the mean stellar mass $B-V$ or the total mass and the amount of coagulation that occurred in galaxies.

When one looks at all this evidence, one can only conclude that the coagulation process is not affected by the physical conditions or the type of stellar clustering. In other words, coagulation is a strictly stochastic process. This conclusion is also supported by the data in Tables 10 and 11, which show that coagulation is, within the limits set by the uncertainties, essentially the same for all types of stellar clusterings.

Apart from the universitality of coagulation, we found that the role of coagulation in the making of the stellar mass spectrum is not detectable after the first 10 million years of existence of the stellar groups, in the sense that it does not in general correlate with other properties of the stellar groups. In other words, the distribution of the number of fragments does not change much in the history of the cluster. The next logical step would then be to study very young stellar groups with reliable age estimates to see how the effects of coagulation on the mass spectrum depend on the physical conditions.

We also think that coagulation (or collisions) might be responsible for the observations of blue stragglers in globular clusters.

Although pure coagulation is generally not a valid approximation of reality, neither is pure fragmentation. The need for dealing with both processes at the same time was again stressed in this work.

We acknowledge financial support by the Conseil de Recherche en Sciences Naturelles et en Génie du Canada (NSERC).

REFERENCES

Aparicio, A., Bertelli, G., Chiosi, C., & Garcia-Pelayo, J. M. 1991, A&AS, 88, 155
Aparicio, A., Garcia-Pelayo, J. M., & Moles, M. 1988, A&AS, 74, 375
Armand, C., Deharveng, L., & Caplan, J. 1992, A&A, 265, 504
Aurière, M., Ortolani, S., & Lauzeral, C. 1990, Nature, 344, 638
Ball, J. M., & Carr, J. 1990, J. Stat. Phys. A. 61, 203
Bastien, P. 1981, A&A, 93, 160
Basu, S., & Rana, N. C. 1992, ApJ, 393, 373
Berkhuijsen, E. M. 1982, A&A, 112, 369
Bhattacharjee, S. K., & Williams, I. P. 1980, A&A, 91, 85
Blackman, J. A., & Marshall, A. 1994, J. Phys. A: Math. Gen., 28, 725
Bounatiro, L., & Arimoto, N. 1992, A&A, 260, 112
Brewer, J. P., Fahlman, G. G., Richer, H. B., Searle, L., & Thompson, I. 1993, AJ, 105, 2158
Brown, J. H., Burkert, A., Truran, J. W. 1991, ApJ, 376, 115
Burki, G. 1977, A&A, 57, 135
Burki, G., & Maeder, A. 1976, A&A, 51, 247
Claudius, M., & Grosbøl, P. J. 1980, A&A, 87, 339
Comeron, F., Rieke, G. H., Burrows, A., & Rieke, M. J. 1993, ApJ, 416, 185
Da Costa, G. S., & Freeman, K. C. 1976, ApJ, 206, 128
Djorgovski, S. 1993, in ASP Conf. Ser. 50, Structure and Dynamics of Globular Clusters, ed. S. G. Djorgovski & G. Meylan (San Francisco: ASP), 373
Dubovskii, P. B., Galkin, V. A., & Stewart, I. W. 1992, J. Phys. A: Math. Gen., 25, 4737
Durrell, P. R., & Harris, W. E. 1993, AJ, 105, 1420
Ellis, R. S., Gondhalekar, P. M., & Efstathiou, G. 1982, MNRAS, 201, 223
Elmegreen, B. G. 1987, in Interstellar Processes, ed. D. J. Hollenbach & H. Thronson (Dordrecht: Reidel), 259
Elmegreen, B. G. 1990, in The Evolution of the Interstellar Medium, ed. L. Blitz (San Francisco: ASP), 247
———. 1991, in NATO ASI Ser. C: Math. Phys. Sci. 342, The Physics of Star Formation and Early Stellar Evolution, ed. C. J. Lada & N. D. Kylafis (Dordrecht: Kluwer), 35
Fahlman, G. G., Richer, H. B., & Nemec, J. 1991, ApJ, 380, 124
Fahlman, G. G., Richer, H. B., Searle, L., & Thompson, I. B. 1989, ApJ, 343, L49
Ferraro, F. R., Fusi Pecci, F., Cacciari, C., Corsi, C., Buonanno, R., Fahlman, G. G., & Ricker, H. B. 1993, AJ, 106, 2324
Ferraro, F. R., & Piotto, G. 1992, MNRAS, 255, 71
Francic, S. P. 1989, AJ, 98, 888
Fusi Pecci, F., Ferraro, F. R., Corsi, C. E., Cacciari, C., & Buonanno, R. 1992, AJ, 104, 1831
Garmany, C. D., Conti, P. S., & Chiosi, C. 1982, ApJ, 263, 777
Habe, A., & Ohta, K. 1992, PASJ, 44, 203
Hambly, N. C., Hawkins, M. R. S., & Jameson, R. F. 1991, MNRAS, 253, 1
Herbst, W., & Miller, D. P. 1982, AJ, 87, 1478
Hesser, J. E., Harris, W. E., VandenBerg, D. A., Allwright, J. W. B., Shott, P., & Stetson, P. B. 1987, PASP, 99, 739
Hillenbrand, L. A., Massey, P., Strom, S. E., & Merrill, K. M. 1993, AJ, 106, 1906
Jeans, J. H. 1928, Astronomy and Cosmogony (Cambridge: Cambridge Univ. Press), 345
Johnstone, D. 1993, AJ, 105, 155
Kamphorst, S. O., & da Silva, J. K. L. 1993, Europhys. Lett., 21, 261
Lada, E. A., Bally, J., & Stark, A. A. 1991a, ApJ, 368, 432
Lada, E. A., DePoy, D. L., Evans, N. J., II, & Gatley, I. 1991b, ApJ, 371, 171

Lada, E. A., DePoy, D. L., Merrill, K. M., & Gatley, I. 1991c, ApJ, 374, 533
Lee, S. W., & Kim, Y. H. 1983, J. Korean Astron. Soc., 16, 43
Lee, H. S., & Lee, S. W. 1984, J. Korean Astron. Soc., 17, 51
Lejeune, C., & Bastien, P. 1986, ApJ, 309, 167
Leonard, P. J. T. 1988, AJ, 95, 108
———. 1989, AJ, 98, 217
Leonard, P. J. T., & Merritt, D. 1989, ApJ, 339, 195
Lin, J.-C. 1992, Phys. Rev. A, 45, 3892
Lyngå, G. 1987, Catalogue of Open Cluster Data (5th ed.; Lund: Lund Observatory)
Massey, P., Garmany, C. D., Silkey, M., & DeGioia-Eastwood, K. 1989a, AJ, 97, 107
Massey, P., & Johnson, J. 1993, AJ, 105, 980
Massey, P., Parker, J. W., & Garmany, C. D. 1989b, A. J. 98, 1305
Masey, P., & Thompson, A. B. 1991, AJ, 101, 1408
Mateo, M. 1988, ApJ, 331, 261
Meylan, G. 1989, A&A, 214, 106
Meylan, G., Dubath, P., & Mayor, M. 1991, ApJ, 383, 587
Miller, G. E., & Scalo, J. M. 1979, ApJS, 41, 51
Nozawa, S., Mizuno, A., Teshima, Y., Ogawa, H., & Fukui, Y. 1991, ApJS, 77, 647
Palla, F., & Stahler, S. W. 1993, ApJ, 418, 414
Paresce, F., et al. 1991, Nature, 352, 297
Parker, J. Wm., Garmany, C. D., Massey, P., & Walborn, N. R. 1992, AJ, 103, 1205
Phelps, R. L., & Janes, K. A. 1993, AJ, 106, 1870
Piotto, G., King, I. R., Capaccioli, M., Ortolani, S., & Djorgovski, S. 1990, ApJ, 350, 662
Pryor, C., & Meylan, G. 1993, in ASP Conf. Ser. 50, Structure and Dynamics of Globular Clusters, ed. S. G. Djorgovski & G. Meylan (San Francisco: ASP, 357
Pryor, C., Smith, G. H., & McClure, R. D. 1986, AJ, 92, 1358
Richer, H. B., & Fahlman, G. G. 1992, Nature, 358, 383
Richer, H. B., Fahlman, G. G., Buonanno, R., & Fusi Pecci, F. 1990, ApJ, 359, L11
Richer, H. B., Fahlman, G. G., Buonanno, R., Fusi, Pecci, F., Searle, L., & Thompson, I. B. 1991, ApJ, 381, 147
Ruprecht, J., Balazs, B., & White, R. E. 1981a, Catalogue of Star Clusters and Associations. I. Associations (Budapest: Publ. House Hungarian Acad. Sci.)
Safranov, V. S. 1963, Soviet Phys.—Dokl., 7, 967
Sagar, R., Piskunov, A. E., Myakutin, V. I., & Joshi, U. C. 1986, MNRAS, 220, 383
Sagar, R., & Richtler, T. 1991, A&A, 250, 324
Saied, E. A., & El-Wakil, S. A. 1994, J. Phys. A: Math. Gen., 27, 185
Salpeter, E. E. 1955, ApJ, 121, 161
Sandage, A. R. 1953, AJ, 58, 61
Sato, T., Richer, H. B., & Fahlman, G. G. 1989, AJ, 98, 1335
Scalo, J. M. 1978, in Protostars and Planets, ed. T. Gehrels (Tucson: Univ. Arizona Press), 265
———. 1986, Fund. Cosmic Phys., 11, 1
Silk, J., & Takahashi, T. 1979, ApJ, 229, 242
Simons, S. 1993, J. Phys. A: Math. Gen., 26, 1259
Sintes, T., Toral, R., & Chakrabarti, A. 1992, Phys. Rev. A, 46, 2039
Smoluchowski, M. 1916, Phys. Z., 17, 557
Sorensen, C. M., Zhang, H. X., & Taylor, T. W. 1987, Phys. Rev. Lett., 59, 363
Spitzer, L., Jr., & Hart, M. H. 1971, ApJ, 164, 399
Straw, S., Hyland, A. R., Jones, T. J., Harvey, P. M., Wilking, B. A., & Joy, M. 1987, ApJ, 314, 283
Straw, S. M., Hyland, A. R., & McGregor, P. J. 1989, ApJS, 69, 99
Taff, L. G. 1974, AJ, 79, 1280
Tarrab, I. 1982, A&A, 109, 285
Trubnikov, B. A. 1971, Soviet Phys.—Dokl., 16, 124
Vázquez, R. A., & Feinstein, A. 1989, Rev. Mexicana Astron. Astrofiz., 17, 3
Vigil, R. D., & Ziff, R. M. 1988, Phys. Rev. Lett., 61, 1431
Wilner, D. J., & Lada, C. J. 1991, AJ, 102, 1050